

**Biodiesel and omega-3 lipids production from the
marine microalgae *Cryptocodinium cohnii***

Emilie Capela dos Santos Daio

Thesis to obtain the Master of Science Degree in

Biological Engineering

Supervisors:

Dr. Maria Teresa Saraiva Lopes da Silva, Ph.D.

Prof. José António Leonardo dos Santos

Examination Committee

Chairperson: Prof. Carla da Conceição Caramujo Rocha de
Carvalho

Supervisor: Dr. Maria Teresa Saraiva Lopes da Silva, Ph.D.

Members of the Committee: Prof. Helena Maria Rodrigues Vasconcelos Pinheiro

November 2021

Preface

The work presented in this thesis was performed at LNEG, Laboratório Nacional de Energia e Geologia (Lisbon, Portugal), and was financed by national funds through FCT - Fundação para a Ciência e a Tecnologia, I.P., within the scope of the project PTDC/EAM-AMB/30169/2017, titled "OMEGAFUEL - New platform for biofuels and omega-3 compounds production, from the marine microalga *Cryptothecodinium cohnii* sustainable biorefinery", during October 2020 - January 2021 (shorter time expected, due to the Covid-19 pandemic lockdown), under the supervision of Dr. Maria Teresa Saraiva Lopes da Silva. The thesis was co-supervised at the Instituto Superior Técnico by Professor José Santos.

I declare that this document is an original work of my own authorship and that it fulfills all the requirements of the Code of Conduct and Good Practices of the Universidade de Lisboa.

Resumo

No presente trabalho procedeu-se ao cultivo da microalga marinha *Crypthecodinium cohnii* ATCC 30772 utilizando um subproduto da indústria do biodiesel – glicerol bruto - de modo a estabelecer-se um protocolo para a obtenção de culturas de elevada densidade celular, em regime descontínuo e semi-descontínuo, com o objetivo de produzir, em simultâneo, ácido docosahexaenóico (ADH) e outros lípidos com potencial aplicação como biodiesel.

Realizaram-se três ensaios (I, II e III) num biorreator de bancada de 7 L. O ensaio I foi realizado em modo descontínuo e os restantes em semi-contínuo (*fed-batch*). O propósito do ensaio I foi estudar as fases de crescimento da microalga (latência, exponencial e estacionária). No ensaio II usou-se um meio de nutrientes concentrado para prolongar a fase de crescimento exponencial da microalga. Contudo, neste ensaio, o crescimento da microalga cessou possivelmente por inibição por substrato e, por outro lado, as partículas do meio interferiram na quantificação da concentração biomassa. Por fim, no ensaio III, diminuiu-se a concentração do meio de alimentação para metade e realizou-se a monitorização do crescimento celular por citometria de fluxo (nº de células/mL), para além do controlo por densidade ótica, tendo sido estabelecidas correlações entre essas leituras e a concentração de biomassa algal por peso seco.

A concentração de biomassa mais elevada foi obtida no Ensaio II, com o valor de 20,82 g/L. A maior produtividade obtida foi também neste ensaio, 1,2 g/(L.h).

No ensaio III, não foi possível obter o teor em lípidos por razões técnicas. No entanto, na experiência II foi possível obter o valor mais alto de lípidos deste estudo, 26,75% p/p biomassa seca. O teor máximo de DHA foi 53,06% p/p ácidos gordos totais, e produtividade máxima em DHA de 0.086 g/(L.h).

Foram ainda estimados parâmetros físicos de uma fração de biodiesel do ensaio II, e todos se enquadraram nos limites definidos pela Norma Europeia EN 14214, de modo a ser usado como combustível.

A citometria de fluxo serviu não só para quantificar o crescimento celular, mas também para analisar a viabilidade das células de *C. cohnii* ao longo dos ensaios.

Palavras-chave: *Crypthecodinium cohnii*; ácido docosahexaenóico (ADH), glicerol bruto; regime semi-descontínuo; biodiesel; citometria de fluxo

Abstract

In the present work the marine microalga *Cryptocodinium cohnii* ATCC 30772 was cultivated using a by-product from the biodiesel industry - crude glycerol - to establish a protocol to obtain cultures of high cell density, in batch and fed-batch regime, with the objective to produce, simultaneously, docosahexaenoic acid (DHA) and other lipids with potential application as biodiesel.

Three experiments (I, II and III) were performed in a 7 L bench bioreactor. Experiment I was performed in batch mode and the others in fed-batch. The purpose of experiment I was to study the growth phases of the microalgae (latent, exponential, and stationary). In experiment II, a concentrated nutrient medium was used to extend the exponential growth phase of the microalgae. However, in this assay, the microalgae growth ceased possibly due to substrate inhibition and, on the other hand, the particles in the medium interfered with the quantification of the biomass concentration. Finally, in experiment III, the concentration of the feeding medium was half reduced, and cell growth was monitored by flow cytometry (cells number/mL), in addition to optical density control, and correlations were established between these readings and algal biomass concentration.

The highest biomass concentration was obtained in experiment II, with the value of 20.82 g/L. The highest productivity was also obtained in this assay, 1.2 g/(L.h).

In the experiment III, it was not possible to obtain lipid content for technical reasons. However, in experiment II it was possible to obtain the highest value of lipids in this study, 26.75% w/w dry biomass. The maximum DHA content was 53.06% w/w total fatty acids, and maximum DHA productivity of 0.086 g/(L.h).

Physical parameters of a biodiesel fraction from experiment II were also estimated, and all met the limits defined by the European Standard EN 14214, to be used as fuel.

Flow cytometry not only served to quantify cell growth, but also to analyze the viability of *C. cohnii* cells throughout the assays.

Keywords: *Cryptocodinium cohnii*; docosahexaenoic acid (DHA); crude glycerol; fed-batch regime; biodiesel; flow cytometry

Acknowledgments

To Dr. Teresa Lopes da Silva, for accepting me in this project, especially in a quite challenging year due to the Covid-19 pandemic. Thank you for your enthusiasm, dedication, expert opinion and kindness.

To Prof. José Leonardo dos Santos for accepting to be my internal supervisor, for everything he taught me in his classes and in the final Biological Engineering Project, and for being a teacher who always encourages us to go beyond horizons.

To all my teachers at Instituto Superior Técnico, for their dedication, encouragement, knowledge, and tools that will certainly help me throughout my life.

To Dr. Alberto Reis for the help and knowledge shared in several aspects of this work.

To Dr. Cristina Oliveira for her help in the analysis of the crude glycerol used in this study.

To all those present at the LNEG at the time I was there, especially Dr. Patrícia Moniz and Carla Dias for all their help, knowledge sharing and motivation.

Finally, to all my friends and family, who were part of my journey, in particular my aunt Elsa Capela for always being there when I needed her most.

Table of Contents

Preface.....	iii
Resumo.....	iv
Abstract.....	v
Acknowledgments.....	vi
Table of Contents.....	vii
List of Figures.....	x
List of Tables.....	xi
List of Equations.....	xii
List of Acronyms.....	xiv
1. Introduction.....	1
1.1. Microalgae Biorefinery Concept.....	1
1.2. The microalgae <i>Cryptocodinium cohnii</i>	5
1.2.1. Morphology and fatty acid biosynthesis.....	5
1.2.2. Growth conditions.....	6
1.2.3. Crude glycerol as low-cost carbon source.....	7
1.3. Docosahexaenoic acid.....	8
1.3.1. Definition and Synthesis.....	8
1.3.2. Industrial Production and Applications.....	9
1.3.3. PUFAs Microbial Production.....	10
1.4. Biodiesel.....	11
1.4.1. Definition.....	11
1.4.2. Third generation biofuel.....	12
1.4.3. Biodiesel Standards.....	12
1.5. Cultivation systems to grow heterotrophic microalgae.....	13
1.6. Flow cytometry.....	14
1.6.1. Equipment.....	15
1.6.2. Enzymatic activity.....	18
1.6.3. Membrane Integrity.....	19
1.6.4. Flow cytometry applications.....	19
1.7. Objectives.....	20
2. Materials and Methods appendix.....	21
2.1. Reagents and Equipment.....	21

2.2.	Experimental strategy	21
2.3.	Strain and Starter Cultures	22
2.4.	Carbon source	22
2.5.	Inoculum	24
2.6.	Cultivation in bioreactor	24
2.7.	Analysis of biomass concentration	26
2.8.	Flow Cytometry.....	26
2.9.	Microscopic Observations	27
2.10.	Nitrogen source and total nitrogen amount determination	27
2.11.	Ash and moisture content determination.....	28
2.12.	Identification and quantification of lipids as total fatty acids (TFA).....	29
2.13.	HPLC	30
2.14.	Kinetic parameters determination.....	30
2.14.1.	Reaction rate	30
2.14.2.	Specific growth rate	30
2.14.3.	Average volumetric productivity.....	31
2.14.4.	Fatty acid composition	31
2.14.5.	Yield.....	32
2.15.	Physical parameters of biodiesel fraction determination	32
2.15.1.	Density	32
2.15.2.	Dynamic and Kinematic Viscosity.....	33
2.15.3.	Cetane number	34
3.	Results and Discussion	35
3.1.	Cultivations	35
3.1.1.	Experiment I.....	35
3.1.2.	Experiment II.....	39
3.1.2.1.	Estimations of Some Physical Parameters of <i>C. cohnii</i> SFA/MUFA Fraction	45
3.1.3.	Experiment III.....	48
4.	Conclusions and Next Steps	53
5.	References.....	55
	Appendix A.....	63
	Appendix B.....	65
	Appendix C.....	66

List of Figures

Figure 1.1 - Schematic representation of a biorefinery generic system.	2
Figure 1.2 - Marine biorefinery from the Status Report Biorefinery 2007.....	3
Figure 1.3 - (A) Representation of <i>C. cohnii</i> (ventral and dorsal view) from Mendes et al. [22]. (B) Photograph of <i>C. cohnii</i> taken in this study (4 days of growth in the bioreactor) under Olympus Corporation microscope at 100x magnification. Larger cells are motionless cysts and motile cells (smaller) are in the surroundings.....	6
Figure 1.4 - Omega-3 fatty acid structure and EPA/DHA synthesis pathway.....	9
Figure 1.5 - Worldwide DHA market application volume by the end of 2012.....	10
Figure 1.6 - Transesterification of TAG with an alcohol (methanol or ethanol), in a presence of a basic catalyst to obtain biodiesel (FAAEs) and glycerol.	11
Figure 1.7 - Schematic representation of different cell target sites and variety of stains for fluorescent labelling used in combination with FC.....	15
Figure 1.8 - Typical flow cytometer schematic representation.....	16
Figure 1.9 - FC controls for population identification.....	17
Figure 1.10 - CytoFLEX (Beckman Coulter Life Sciences, USA) WDM Optical Filter Display Colour Codes, channel bandpass (BP) filters names and commonly used fluorescent dyes.....	18
Figure 2.1 - Experimental strategy development (experiments I, II and III) carried out during the present work.....	21
Figure 2.2 - Bioreactor and controller module used in the experiment (left); schematic representation with main bioreactor dimensions (right).....	25
Figure 3.1 - <i>C. cohnii</i> ATCC 30772 growth in batch mode (experiment I).....	35
Figure 3.2 - Percentage of cells in each subpopulation, as defined in Introduction Flow cytometry chapter, for Experiment I.....	39
Figure 3.3 - <i>C. cohnii</i> ATCC 30772 growth in fed-batch mode (experiment II).....	40
Figure 3.4 - Percentage of cells in each subpopulation for Experiment II.....	48
Figure 3.5 - <i>C. cohnii</i> ATCC 30772 growth in fed-batch mode (experiment III).....	49
Figure 3.6 - Percentage of cells in each subpopulation for Experiment III.....	51

List of Tables

Table 2.1 - Composition of the crude glycerol supplied by Iberol (Alhandra, Portugal), used in experiments I and II	23
Table 2.2 - Composition of the crude glycerol supplied by Iberol (Alhandra, Portugal), used in experiment III.....	23
Table 3.1 - Kinetic parameters calculated for <i>C. cohnii</i> growth in Experiment I, according to the equations shown in the Materials and Methods Section.....	37
Table 3.2 - Fatty acid composition, as percentage of total fatty acids (%w/w TFA), obtained for assay I concerning <i>C. cohnii</i> ATCC 30772, grown in batch mode. Data represent the mean of two analyses (two independent samples, injected once).....	38
Table 3.3 - Kinetic parameters calculated for <i>C. cohnii</i> growth in Experiment II, according to the expressions shown in the Materials and Methods Section	42
Table 3.4 - Fatty acid composition, as percentage of total fatty acids (% w/w TFA), obtained for <i>C. cohnii</i> ATCC 30772, grown in fed-batch mode. Data represent the mean of two analyses (two independent samples, injected once over time (h)).....	44
Table 3.5 – <i>C. cohnii</i> SFA+MUFA fraction , FA composition, weight percentages (w_i), normalized molar fractions (x_i) and molecular weights (MW _i) [94]......	45
Table 3.6 - Parameters A, B and C [83], along with the temperature-dependent molar volume for each group considered in a FAME at 288 K (15 °C) and 313 K (40 °C).....	46
Table 3.7. Number of groups for each of the considered groups corresponding to each fatty acid in the biodiesel fraction.....	46
Table 3.8. Parameters A, B and T ₀ considered for each of the FAMEs present in the biodiesel fraction.	47
Table 3.9 - Kinetic parameters calculated for <i>C. cohnii</i> growth in Experiment III, according to the expressions shown in the Materials and Methods Section.	50
Table A.1 - Chemical reagents used in this work.....	63
Table A.1 (continuation) - Chemical reagents used in this work.....	64
Table A.2 - Requirements of biodiesel properties according to the European standard EN 14214	66
Table A.2 (continuation) - Requirements of biodiesel properties according to the European standard EN 14214.....	67

List of Equations

Equation (1) – Total nitrogen content (%). V , HCl (0.1 N) volume in mL spent in the sample titration, and m is the sample mass, in grams.	28
Equation (2) - Moisture content (%). m is the weight of calcined crucibles (after oven 100 °C)	28
Equation (3) – Ash content (%) . The crucibles were placed in a muffle furnace at 550°C for 1 h, cooled in a desiccator and weighed.	28
Equation (4) - Quantification of the fatty acids. m_{FA_i} is the mass of fatty acid i , A_{FA_i} is the area of the fatty acid peak, $A_{(17:0)}$ is the area of the peak corresponding to the internal standard and RF_{FA} is the response factor of the fatty acid FA_i	29
Equation (5) – Reaction rate, r_i . ΔC_i is the concentration variation in the Δt , which is the time interval corresponding to C_i variation	30
Equation (6) - Specific growth rate (μ_{max}) in h^{-1} . DCW_0 is the dry cell weight in the moment of the inoculation.....	30
Equation (7) - Average volumetric productivity of A in a time t ($P_{A\ average}(t)$). C_A is the concentration of A at time t ($C_A(t)$) and at t_0 ($C_A(t_0)$), the initial time ($t = 0$)	31
Equation (8) - Percentage of each fatty acid in the total mass of fatty acids % TFA $_i$ (W_{FA_i}/W_{TFA}). % FA_i (W_{FA_i}/W_{TFA}) is the percentage of fatty acid i , m_{FA_i} is the mass of fatty acid i and m_{TFA} is the total mass of fatty acids	31
Equation (9) - Lipid content (TFA), in % TFA (W_{FA}/W_{TFA})	31
Equation (10) - Total fatty acid productivity (P_{FA}), P_x is the average volumetric biomass productivity and %TFA ($W_{TFA}/W_{biomass}$) is the percentage of total fatty acids relative to biomass	31
Equation (11) - Yield between two substances A and B ($Y_{A/B}$) , i.e, the ratio between A formation rate (r_A) and B consumption rate (r_B) for the same period Δt	32
Equation (12) - Density, ρ , in which the molecular weight, MW_j , and molar volume, V_j , are related, and x_j corresponds to the molar fraction of component j	32
Equation (13) - Molar volume, V_j , of a component j , n_i is the number of group i , and ΔV_i is the temperature dependency of the molar group in cm^3/mol ; T is temperature in Kelvin and A_i , B_i and C_i are fixed parameters of each chemical group.	32
Equation (14) - Dynamic viscosity, μ_d , that correlates the density, ρ , and kinematic viscosity, ν	33
Equation (15) - Viscosity of a liquid mixture, μ_m , in which x_i is the mole fraction of component i , and μ_i the viscosity of each pure FAME in mPa.s	33

Equation_(16) - Relationship between temperature and μ_t . A, B, C and T_0 are parameters obtained by fitting real data	33
Equation_(17) - Cetane number, CN with DU as the degree of unsaturation and SCSF is the straight-chain factor	34
Equation_(18) – DU, with w_i as the weight percentage of each FAME and n is the total number of double bonds it contains.....	34
Equation_(19) - SCSF, with MW_i as the molecular weight of each saturated FAME	34
Equation_(20) – Correlation between optical density at 470 nm, OD_{470} , and cell number, cells/mL ..	65
Equation_(21) – Correlation between dry cell weight, DCW (g/L) and cell number, cells/mL	65
Equation_(22) - Correlation between dry cell weight, DCW (g/L) and optical density at 470 nm, OD_{470}	65

List of Acronyms

12:0	Lauric acid
14:0	Myristic acid
16:0	Palmitic acid
18:2ω6	Linoleic acid
18:2ω9	Oleic acid
ALA	α -linolenic acid
APIs	Active Pharmaceutical Ingredients
<i>C. cohnii</i>	<i>Cryptocodium cohnii</i>
CDS	Chromatography Data System
CFDA	Carboxyfluorescein diacetate
CFUs	Colony forming units
CHP	Combined heat and power
CN	Cetane Number
CSL	Corn Steep Liquor
DAD	Diode Array Detector
DCW	Dry cell weight
DHA	Docosahexaenoic acid
DO	Dissolved Oxygen Percentage
DU	Degree of Unsaturation
EPA	Eicosapentaenoic
EPS	Extracellular Polysaccharide
FAAEs	Fatty acid alkyl esters
FACS	Fluorescence-activated cell sorting
FAMEs	Fatty acid methyl esters
FAs	Fatty acids
FC	Flow cytometry

FFA	Free fatty acids
FID	Flame Ionization Detector
FSC	Forward scatter
GC	Gas Chromatography
GHE	Greenhouse effect
HPLC	High-Performance Liquid Chromatography
IEA	International Energy Agency
LC-PUFAs	Long-chain polyunsaturated fatty acids
MUFAs	Monounsaturated fatty acids
NaNO₃	Sodium Nitrate
NGOM	Non-Glycerol Organic Matter
OD	Optical Density
PI	Propidium iodide
PUFAs	Polyunsaturated fatty acids
SCO	Single Cell Oil
SCSF	Straight-Chain Factor
SSC	Side scatter
TAGs	Triacylglycerols
THF	Tetrahydrofuran
WDM	Wavelength Division Multiplexer
ω-3	Omega-3

1. Introduction

1.1. Microalgae Biorefinery Concept

Currently, the energy demand worldwide is strongly dependent on fossil fuels and their derivatives consumption, which contributes for the greenhouse effect (GHE) increase, and the fossil reserves exhaustion, in a near future [1]. As a result of the global energy requirements imbalance, a massive pressure is being applied on the purchase prices levels, coupled with environmental problems and political concerns [2]. An attempt to meet the increasing energy demand in a sustainable way consists of using renewable bio-based resources to produce materials and energy [3]

Similar to common petroleum refinery where fossil fuels are the input to produce energy, biorefineries are green energy systems that use as an input biomass to produce several products, including biofuels, using a combination of technology and processes [1]. The sources of biomass are diverse, from agriculture, forestry and aquaculture, including industry and households wastes such as wood, forest residues, organic residues, both animal and plant derived, agricultural crops, and aquatic biomass (algae and seaweeds) [3].

Kamm and Kamm [4] described three types of biorefineries: the 'whole crop biorefinery' that used as an input raw materials such as maize and wheat; the 'green biorefinery', using natural wet feedstocks such as grass, green crops or immature cereal (essentially untreated products); and the 'lignocellulose feedstock biorefinery' using dry biomass or waste containing cellulose, that is later broken down in hemicellulose, cellulose, and lignin. The Status Report Biorefinery 2007, by Ree and Annevelink [5] attributes, among the biorefineries types described above, biorefinery classification focused on the technologies involved: the thermochemical, conventional and two-platform concept biorefineries that combines the sugar platform (biochemical conversion) and with the syngas platform (thermochemical conversion).

The International Energy Agency (IEA) was created in 1978, to increase information exchange and cooperation between countries that have national projects regarding bioenergy research, development, and implementation [6]. In 2008, IEA Bioenergy Task 42 developed an appropriate biorefinery classification from biomass to end-products chains focusing on the large-volume production of biofuels for the transportation sector, according four key elements: feedstocks, processes, platforms, and products (Figure 1.1) [3]. The development of biorefinery complexes is the combination of these four features and some guidelines must be achieved to produce at least one high value product, oriented in the continuous feedstocks refining; and the production of at least one biofuel (liquid, solid or gaseous) is desirable, a part of heat and electricity [2].

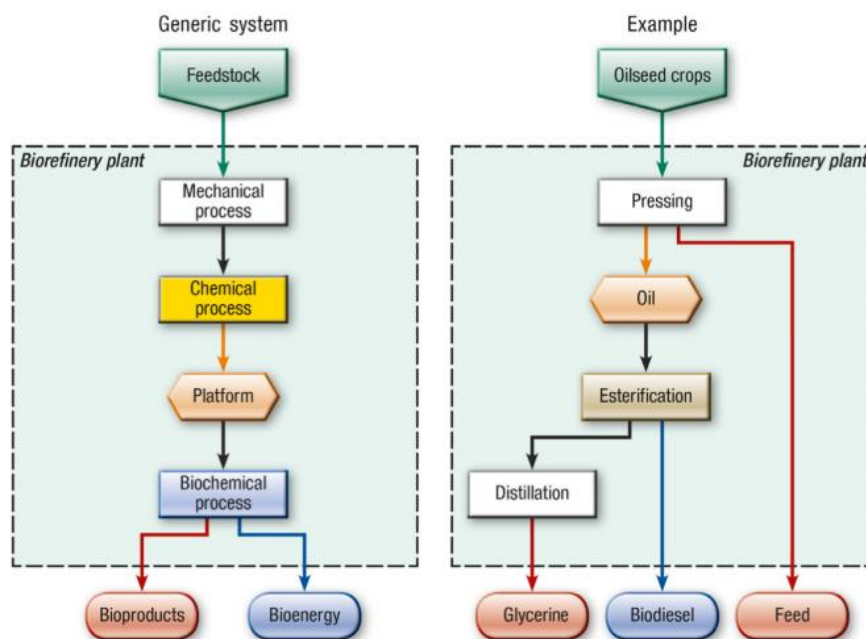


Figure 1.1 - Schematic representation of a biorefinery generic system. On the left is described a conversion pathway from feedstock to products, via processes and platforms (intermediates from which final products are derived). On the right, an example of a biorefinery plant representation, from oilseed crops pressing, oil is used to produce glycerine and biodiesel via an esterification reaction [3].

The potential of marine biomass has been progressively investigated, due to its enormous resource dimension. Nearly three to four quarters of planet earth's surface is water and the world population benefit from these aquatic resources, that include a substantial biodiversity covering both fresh and marine environments where 80% of existing living beings are found [7].

So far, terrestrial biomass-based biorefineries have been the focus of administrations for energy crop cultivations, slightly considering marine crops, i.e. macroalgae (green, brown and red), also known as seaweeds, and microalgae (green, golden, blue algae and diatoms) [5][7]. However, life cycle of terrestrial biomass final products are exacerbating climate change, as GHE is increasing, high carbon debt is induced, water is highly consumed and there is also a competition with food industry [8] and land usage [7]. Moreover, macro- and microalgae are an alternative to lignocellulosic feedstocks for the production of biofuels, since they lack or have a low amount of lignin in their chemical structure [9].

The type of algae chosen and growth parameters, determine the bio-based products that these organisms can produce such as starch, oils, vitamins, and carbohydrates. In Figure 1.2, a marine biorefinery is schematically represented, including major paths for products obtention, some of them above mentioned and, in terms of energy efficiency, combined heat and power (CHP) can also be obtained. Lastly, from an environmental point of view, autotrophic microalgae by converting solar energy into biomass and oils contribute for GHE mitigation, given their capacity to consume carbon dioxide (CO₂).

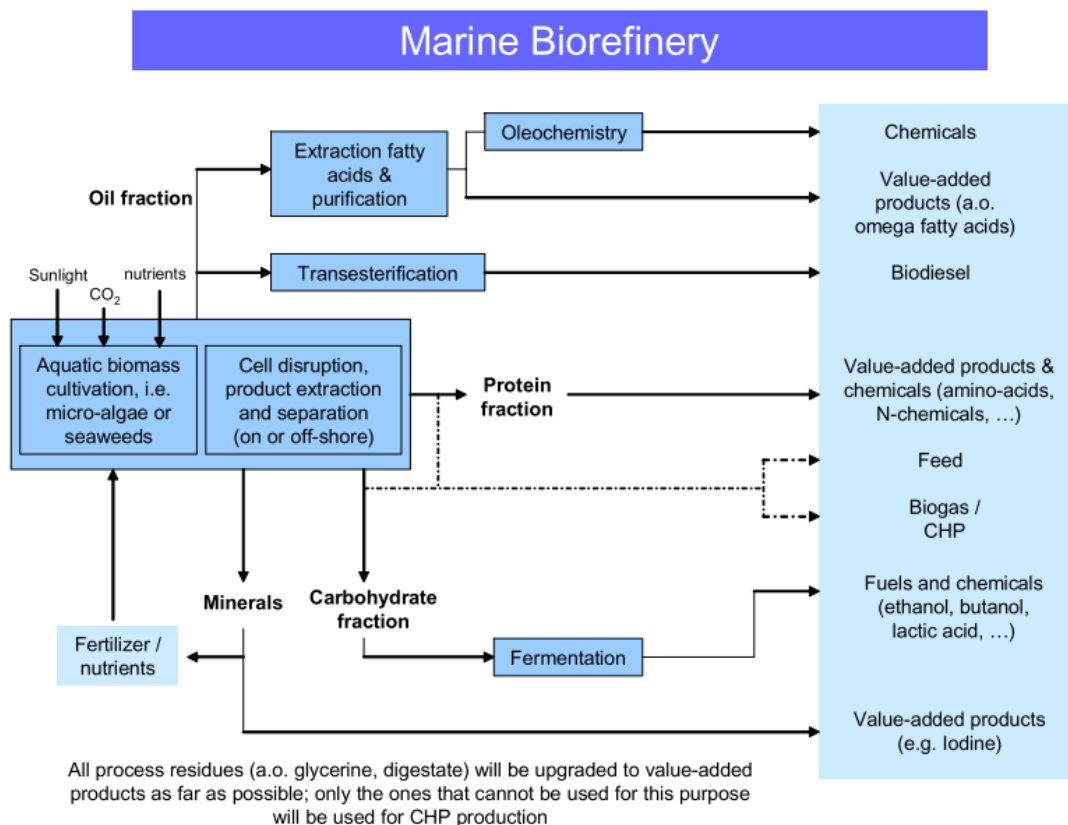


Figure 1.2 - Marine biorefinery from the Status Report Biorefinery 2007 [5].

Although the economic and environmental distinction of macroalgae, enhanced by the endeavours investigation, there are still many gaps since macroalgae are particularly exceptional from terrestrial biomass as they have unique carbohydrates which implies new technologies apart from the ones used in terrestrial biomass-based biorefineries [8]. This is even more expressed in European nations that have less knowhow compared to Asia ones, and it has been imperative to thoroughly review studies regarding the integrated processes of marine macroalgae-based biorefinery [9].

Biotransformations and biorefineries built on microbial biomass are an alternative to produce biofuels diminishing the environmental impacts already mentioned. However, the main bottleneck of its commercialization is the high production cost. Therefore, to overcome this challenge, strategies are being implemented to increase the monetary value of the whole process, by taking advantage of the various coproduced products and microbial biomass components that are economically competitive, also using low-cost feedstocks such as industrial by-products or effluents, as an integrated process that aims at waste reduction [10].

In this way, several studies have shown the potentially sustainable growth media for microalgae and bacteria dual systems for wastewater treatment. J. Olguín [11] designed a municipal wastewater treatment plant with oleaginous microalgae recovery, combined with *Arthrospira (Spirulina)* that was cultivated in seawater supplemented with piggery waste for

anaerobic digestion that led to the production of biogas, hydrogen, biodiesel and other valuable compounds. Albeit the fairly minor scale applications of microalgae in wastewater treatment, many species have the major requirement which is the ability to use abundant inorganic nitrogen (N), phosphorous (P) and organic carbon in the effluents content, making them even more attractive [12].

So far, other microbial producers may also contribute to the biorefinery concept since they also intracellularly produce compounds that are marketable. Marcelino *et al.* [13] proposed an alternative to lignocellulosic biorefinery using 27 types of yeasts to produce biosurfactants, having antimicrobial and antitumor properties, alongside with the advantage of high biodegradability and low toxicity, on the basis use of sugarcane bagasse hemicellulosic hydrolysate as carbon source. Regarding bacteria, genetic engineering by optimizing genetic and regulatory processes that change metabolic pathways, oil and chemical accumulation can be improved [10].

Microalgae are one of the earliest forms of life and have some peculiarities that make them the most studied microorganisms for microbial biorefineries. The ecological habitats where microalgae can be found are diverse, which make them able to thrive in numerous extreme environments in terms of pH and temperature [14]. Furthermore, many microalgae are single-cell organisms, and they can grow fast in raceways as continuous culture systems, or in bioreactors. In addition, the process productivity can be improved by changing the growth and harvesting conditions [14]. There are many autotrophic microalgae based biorefineries reported in literature [15][16][17]. However, autotrophic microalgae cultivation systems present a few bottlenecks: (i) the microalgae growth is light-dependent, requiring expensive and specific equipment design; (ii) for an efficient conversion, the culture media are usually treated in large volumes, in photobioreactors, in which light penetration into the dense cultures is hindered due to the self-shading effect; (iii) as a result, the microalgae cell concentration in the culture is usually low, due to the inefficient light penetration, aggravated by the light shading effect. In addition, microalgae grown under autotrophic conditions usually produce low amounts of intracellular products, such as lipids and pigments, due to the low biomass concentrations and productivities. Moreover, autotrophic microalgae growth is affected by temperature and light availability; hence, this technology is not suitable in areas of high latitude, where most seasons have low temperature and fewer daylight hours, as the European Northern countries [18].

On contrary, heterotrophic microalgae use organic compounds as carbon and energy sources to grow and do not use light as an energy source. Indeed, these microorganisms show several benefits over the autotrophic microalgae such as: (a) they can grow in cheaper conventional bioreactors, requiring less sophisticated equipment, and are, therefore, easily scaled-up; (b) they do not require light to grow, which reduces the equipment requirements and costs; (c) the cultures attain higher, denser cell concentrations and intracellular product productivities than autotrophic cultures; (d) the algal biomass composition can be tailored by changing the type of organic substrate in the medium; (e) heterotrophic microalgae can remove

organic carbonaceous, nitrogen, and phosphorus compounds from the wastes more efficiently than autotrophic growth [18].

At a commercial scale, there are no reports on the biorefinery concept applied to heterotrophic microalgal biomass, despite its potential to obtain lipids for biodiesel or bioenergy production, and ω -3 fatty acids, which have several applications for pharmaceutical, nutraceutical and food purposes.

1.2. The microalgae *Cryptocodinium cohnii*

1.2.1. Morphology and fatty acid biosynthesis

Cryptocodinium cohnii (*C. cohnii*) (Figure 1.3) is a marine dinoflagellate, heterotrophic and unicellular microalgae that is part of a species complex, with numerous isolated species siblings morphologically very analogous, that can be found worldwide in temperate and tropical waters [19]. Some strains of *C. cohnii* grow axenically in an organic medium, however, in nature they are often phagotrophic strains present among macrophytes, predominantly *Fucus* spp., or other decaying seaweeds, having a typical myzocytosis food uptake mechanism [20].

The reported phenotypic characteristics of the cells separate them in two forms, non-motile cysts, and swimming cells. The motile swimming cells have two flagella, one is flattened and gives the cell spinning and propulsive force; and other flagellum that acts like a rudder for steering is directed posteriorly along a longitudinal groove [21]. The cysts, with an ovoid shape, can be vegetative and divide into 2, 4 or 8 daughter cells, or stay in a dormant stage [21].

C. cohnii is an oleaginous organism, and it is known by the ability to produce and accumulate lipids with a high fraction of docosahexaenoic acid (DHA), a polyunsaturated fatty acid (PUFA), part of ω -3 group (22:6). The peculiarity of this microalgae is related with the fact that no other PUFAs are produced in significant amount, which facilitates the downstream DHA purification step, and makes attractive the industrial production [21].

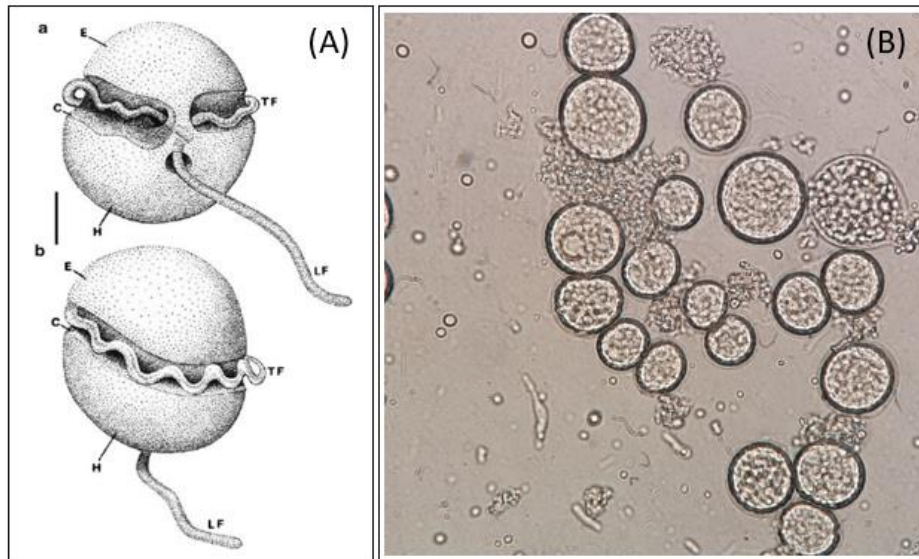


Figure 1.3 - (A) Representation of *C. cohnii* (ventral and dorsal view) from Mendes *et al.* [22]. (B) Photograph of *C. cohnii* taken in this study (4 days of growth in the bioreactor) under Olympus Corporation microscope at 100x magnification. Larger cells are motionless cysts and motile cells (smaller) are in the surroundings.

The total lipid content accumulated can exceed more than 20% of biomass dry cell weight (DCW), depending on the growth conditions [23], [24]. Fatty acids (FAs) biosynthesis culminates in the formation of C16 or C18 saturated FAs in a first phase, subsequently they are converted to monounsaturated FAs and 22:6 ω -3 (*de novo* synthesis) through a series of desaturases and elongases resulting in an extended range of PUFAs. While 70% are neutral lipids and characterized as triacylglycerols (TAGs) rich in DHA (over 30% of total fatty acid content), the remaining are polar lipids [24][22].

In addition to DHA, *C. cohnii* fatty acid profile reports include lauric acid (12:0), myristic acid (14:0), palmitic acid (16:0), 18:2 ω 6 (linoleic acid) and 18:2 ω 9 (oleic acid) as common fatty acids [22], [23], [25], [26]. The distribution of these fatty acids between the neutral or polar fractions is dependent on the strain of *C. cohnii* and the respective cultivation stage, mainly at nutrient limitation [26].

1.2.2. Growth conditions

Several efforts have been made to study the optimal growth conditions for lipid accumulation.

Considering the carbon source, studies demonstrate that the microalgae is able to grow in different media composition, containing ethanol, pure glycerol, acetic acid (acetate), glucose, sucrose, galactose or mannose [26][27][28][29]. Positive results were also obtained with other complex sources, such as rapeseed meal hydrolysate mixed with waste molasses (two agro-industrial by-products) [30], carob pulp syrup [31], cheese whey with corn steep liquor [32] and

crude glycerol [33]. No growth was observed in maltose, arabinose, rhamnose, galacturonic acid, aldose and fructose [22].

The most common used substrate for lipid production is glucose [34]. However the production in large scale bioreactors is compromised by the fact that in this medium *C. cohnii* produces an extracellular polysaccharide (EPS) that increases substantially the culture viscosity, blocking the oxygen supply to be satisfied during the process reducing the overall volumetric productivity of DHA [29]. An attempt to overcome this limitation could be a vigorous stirring. However it has been reported that mechanical agitation affects dinoflagellates with slower growth rates [22].

The sources of nitrogen provided to the culture medium are likewise diverse, including the complex ones already mentioned (waste molasses and corn steep liquor) and others such as yeast extract, peptone, meat extract, glutamic acid, ammonium chloride (NH_4Cl) and potassium nitrate (KNO_3) [22][35].

Natural seawater would be the best option regarding inorganic salts, but artificial seawater may be considered, containing NH_4HCO_3 (ammonium hydrogen carbonate), $(\text{NH}_4)_2\text{SO}_4$ (ammonium sulphate), NaNO_3 (sodium nitrate) or $(\text{NH}_2)_2\text{CO}$ (urea), in addition other salts can be used (phosphate and magnesium salts) and some heavy metals (such as iron, cobalt and zinc), all inexpensive nutrients [22]. The salinity range ideal for cultivations is 16 to 29 g/L of sodium chloride, having no impact of growth in this interval, but for large scale production low sea salts concentrations are preferable to avoid corrosion problems [36].

Temperature and pH are additional key factors for microalgal growth and product synthesis. Safdar *et al.* [37] described the range of temperature between 25 and 30 °C as optimal, and pH ranges from 6 to 7, with a maximum growth rate obtained for pH 6.5. Although in some studies these ranges differ with the strain cultivated, and in industrial production where cooling systems are implemented, strains that grow at higher temperatures ranges are preferable, since they have a faster doubling time, which leads to an overall reduction in fermentation time [22][38]. The agreement among studies is that light is an inhibitory parameter since growth accelerates in the dark [22].

1.2.3. Crude glycerol as low-cost carbon source

Crude glycerol ($\text{C}_3\text{H}_8\text{O}_3$) is the main by-product of biodiesel production and with the increase of interest in this biofuel worldwide combined with sustainability issues. Crude glycerol price has decreased being essential to manage its production, in order to have a zero-waste disposal [39].

Comparing to hydrocarbons obtained in traditional petrochemical refineries, glycerol is highly functionalized molecule that can be directly used as an alternative feedstock for numerous processes, including for the production of DHA and other lipids by heterotrophic microalgae,

reducing the cost of biodiesel commercial production [40]. Crude glycerol is highly viscous, dark brown colour and alkaline pH, and it is effectively half of glucose ($C_6H_{12}O_6$), therefore the metabolic pathway chosen by the cells for this substrate is the same (glycolytic pathway) [40][41].

However, there is a limitation regarding crude glycerol application in certain species since not all heterotrophic microalgae can use this carbon source. Abad *et al.* [42] presented an overview of growth and DHA yields obtained from three microorganism, *Thraustochytrium*, *Schizochytrium*, *Aurantiochytrium* and for their strains variations, and concluded that microalgae grown on crude glycerol as a carbon source can grow with similar yields to pure glycerol or glucose.

Da Silva *et al.* used low-carbon sources substrates (sugarcane molasses, vinegar effluent and crude glycerol) for *C. cohnii* ATC 30772 lipids production in 500 mL shake-flasks cultures. Crude glycerol produced the highest lipid and DHA content (14.7% w/w DCW and 6.56 mg/g, respectively) [33].

Nevertheless, crude glycerol purity varies from 20% to 80% according to the biodiesel production process stages (catalytic and purification processes) and particularities such as raw materials used, consisting in a mixture of water, methanol, ash, NaCl, soap and others [41]. Despite of the low-cost of this substrate, cells metabolism can be affected by inhibitory compounds present in crude glycerol, therefore declining the process yield. Sarma *et al.* reported an example of inhibitory effects of glycerol impurities in *Enterobacter aerogenes* bacterium, concluding that metabolism was highly disturbed by methanol and soaps [39].

1.3. Docosahexaenoic acid

1.3.1. Definition and Synthesis

Docosahexaenoic acid (DHA, 22:6) is an omega-3 (ω -3 or n-3) long-chain polyunsaturated fatty acids (LC-PUFAs) that are found in large amounts in the human brain and the heart. However it can also be present in other tissues having important functional effects [43]. PUFAs classification is according to the position of the first double bond counting from the methyl terminus, and DHA has its first one at position 3, having a total of 6 double bonds from a backbone with 22 carbon atoms in overall.

Due to the lack of DHA *de novo* synthesis in mammals, alternatives for its obtention depend on dietary supply, especially the intake of fish and, in children, also breastfeeding. [44]. Marine food chains are rich in DHA and EPA (eicosapentaenoic, 20:5 n-3), so fish and seafood are the major dietary source of LC-PUFAs as a result of an accumulation in their diet, but fish oil or fishmeal are limited sources due to global fisheries maximum exploitation [45].

The pathway of EPA and DHA synthesis has α -linolenic acid (ALA, 18:3 n-3) as precursor, and include a series of desaturases and elongases activity (Figure 1.4). In humans, studies show that ALA bio-conversion into EPA and DHA is rate limiting [46], and this is even more striking in vegetarian or vegan diets, increasing the need of compatible sources, such as algae oil as dietary supplement.

Algae and microalgae, including *C. cohnii*, are direct producers of these two PUFAs and are currently being used and formulated for fish farms and for human consumption, and are currently in the market by different industries [47]. Microalgae have the peculiarity of producing singular PUFAs that are easily extracted and purified. In addition, they are cholesterol free, taste good and are odourless [22].

Emphasis on omega-3 supplementation for human health is growing, since DHA is incorporated into phospholipids membrane in the brain, playing a vital role in prenatal and postnatal development, cognitive development, learning and memory; it reduces the risk of neuropsychiatric disorders as well as visual injuries, since it is also present in high concentrations in the retina [22][48]. EPA and DHA appear to be involved in antiangiogenic activities, with antitumoral and anticancer properties [49]; they also prevent diabetic complications and obesity conditions [50].

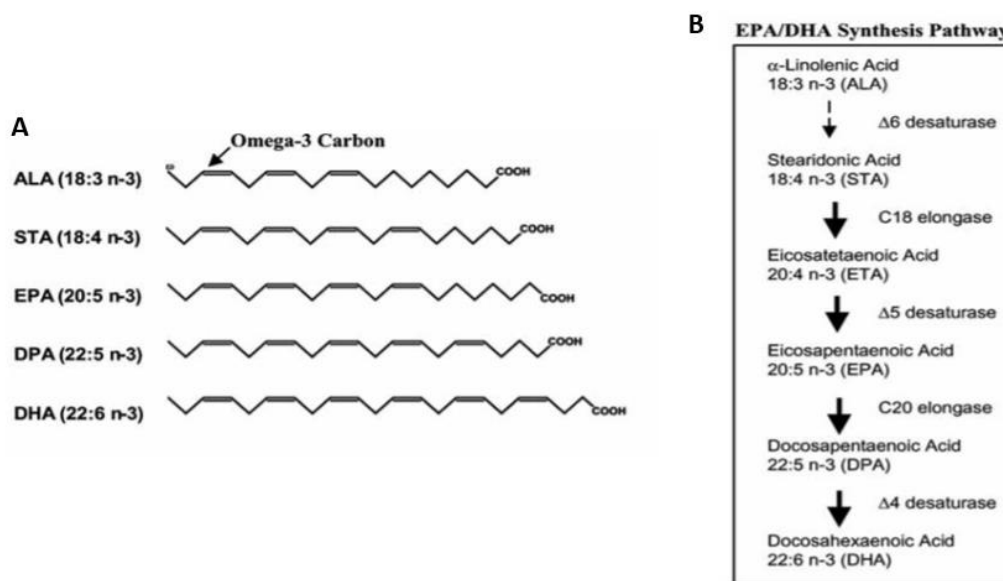


Figure 1.4 - Omega-3 fatty acid structure and EPA/DHA synthesis pathway. Adapted from Doughman *et al.* [40].

1.3.2. Industrial Production and Applications

In the early 1990s PUFAs production, mostly DHA and EPA, gained expression in aquaculture for nutritional feeding enrichment purposes and, with the increasing awareness of

their benefits in human health, they became part of Active Pharmaceutical Ingredients (APIs), enriching in first place supplements for infants consumption, and later extended for adults [21].

C. cohnii is valorised and commercialized for poultry, ruminants and other animals feed to produce, for example, eggs and milk rich in omega-3 [47]. Since the major application are for human or animal consumption, their manufacture must follow a range of regulations and standards, having a high overall cost of production that can be diminished by biorefinery strategies as mentioned before [51].

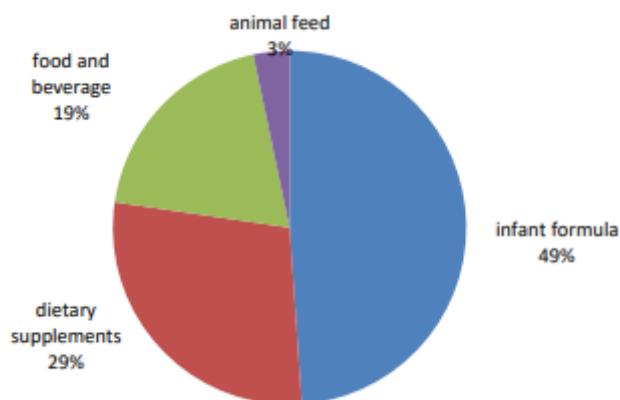


Figure 1.5 - Worldwide DHA market application volume by the end of 2012, adapted from der Voort *et al.* [52].

These commercial facilities are distributed worldwide and are dominated by Asia and North America [51], and the major supplier is DSM Enterprises (comprising Martek Biosciences Corporation), with DHASCO™ oil infant formula (40-50% of DHA) produced by *C. cohnii* for nutritional purposes [21]. In 2014, the global omega-3 value was around 320 million €, and its applications distribution for DHA oil in 2012 is in Figure 1.5 [52].

1.3.3. PUFAs Microbial Production

So far, a few wild-type microorganisms are qualified to produce PUFAs containing more than 20 carbon atoms, and this group includes fungi, marine microalgae, and bacteria. With a couple of exceptions, bacteria are not the most important single cell oil (SCO) producers, since its accumulation is minimal [29]; alternatively, fungi such as *Rhodospiridium toruloides* was found to yield 100 g/L biomass and accumulate 50-70% of lipids of its total DCW, making it a potential feedstock for oleochemicals and biofuels production [53].

Indeed, a robust strain that is able to grow on various carbon sources and has a high inhibitor tolerance leads to increased lipid production and, in the future, genetic engineering may be the answer combined with random mutagenesis [53].

Lipid accumulation is a dynamic process that depends on the microorganism and the growth conditions. Therefore, some strategies involve separating the cultivation into two phases: biomass production and lipid accumulation. *C. cohnii* starts to accumulate oil in the stationary phase or during growth-limiting conditions when cells are under stress. It has been reported that *C. cohnii* DHA production is negatively affected by increasing lipid concentration, thus maximum growth and maximum DHA accumulation occur for different culture media [22].

1.4. Biodiesel

1.4.1. Definition

Fatty acid alkyl esters (FAAEs), commonly known as biodiesel, is an ecologically friendly fuel that is an alternative to diesel fuel or extender. Biodiesel is derived from renewable feedstocks, such as animal fats, vegetable oils (edible and non-edible oils) or waste (recycled oils) [54][55][56]. These feedstocks are composed of triacylglycerols (TAGs) containing a LC-PUFA chemically bound to a glycerol backbone.

The common process to convert TAG into biodiesel is through a reaction between TAG and an alcohol in the presence of a catalyst at high temperature - transesterification reaction - resulting in a mixture of FAAEs and glycerol (Figure 1.6), product by-product already referred (Section 1.2.3) [54][56]. The alcohol used in the transesterification reaction determines the type of FAAEs obtained; when using methanol, the most common alcohol utilized, and using an alkali catalyst, FAMEs (fatty acid methyl esters) are obtained; besides methanol, other alcohols may also be used for biodiesel preparation, such as ethanol, butanol, propanol, and iso-propanol [56].

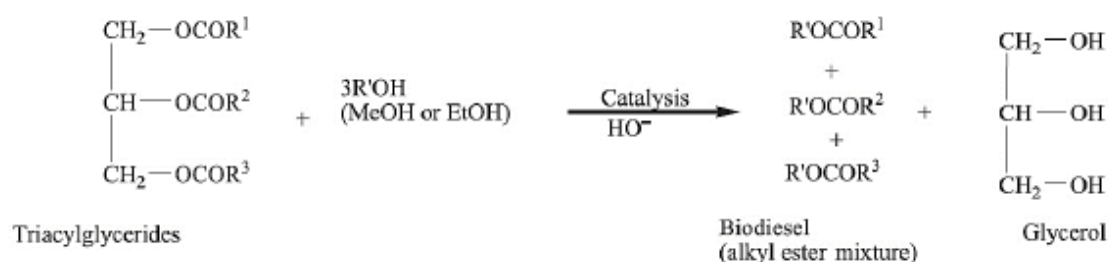


Figure 1.6 - Transesterification of TAG with an alcohol (methanol or ethanol), in a presence of a basic catalyst to obtain biodiesel (FAAEs) and glycerol. Reproduced from Naik *et al.* [54].

Homogeneous alkaline base catalysts are commonly used in the commercial biodiesel production for being less expensive. However, the catalyst choice (basic or acidic) should consider the feedstock quality in terms of the presence of free fatty acids (FFA). Acidic catalysts are recommended for high FFA amounts and basic catalyst otherwise, to avoid FFA and alkali catalyst side reaction that forms soap and water [54][57].

Methanol is not soluble in oil (TAG) and initially two immiscible phases are formed, in which the catalyst assists to increase solubility. However, the use of co-solvents such as tetrahydrofuran (THF) accelerates the production of FAMEs, transforming the two phases into one and the reaction takes place [56].

1.4.2. Third generation biofuel

Recently, microalgae have emerged as the third generation of biodiesel feedstock, as a replacement of other renewable fuels that compete for land use and with the food industry.

Conventional feedstocks for first generation biofuels are those derived from food crops, such as oilseeds for biodiesel, sugar (sugar beet, sugarcane, and sweet sorghum) and starch crops (wheat and corn) to produce bioethanol through fermentation steps. Regarding vegetable oils for biodiesel production by transesterification, the most common used are rapeseed oil, soybean oil, palm oil, and coconut oil, distributed globally and in 2015 they accounted 69% of total biodiesel output [58]. Nevertheless, these edible feedstocks have social impacts, in food supply and prices, besides environmental concerns with the reduction in water and soil quality, leading to a search for alternative sources for the biodiesel production [59][60].

The second-generation biofuels are derived from non-food lignocellulosic material such as agricultural, forest and municipal wastes. In this group, the production has a seasonal nature, for plants like *Jatropha*, *Jajoba* and *Karanja*; or other obstacles related with pre-processing, storage and transport, which contributes for the production cost increase [59].

Microalgae show benefits over other feedstock due to their harvestability as they can double their biomass in 24 hours, having higher productivity and fermentation yields. The main limitation to commercial development is microalgae cultivation, and it has been addressed by many researchers, also to improve downstream processing, conversion, and extraction techniques [60].

1.4.3. Biodiesel Standards

The increase in biodiesel production observed in the past several years, driven by concerns on petroleum reserves and environmental issues, led to the establishment of relevant characteristics standards to be in line with existing engines. Important fuel criterium for biodiesel use as diesel fuel substitute has to guarantee that transesterification final products have no residual chemicals (FFAs, alcohol or catalysts), also biodiesel properties such as density, viscosity, flash-point, cetane number, and others must be in specified intervals [55][61][62][58].

Biodiesel fuel in FAME form is now manufactured in many countries. In the United States the relevant standard for biodiesel characterization is ASTM D6751, while in Europe EN 14214 is

a separated standard valid to the automotive sector and EN 14213 for heating purposes [62]. Several properties are shown in Table A.1 according to EN 14214 standard [63].

Another property related with FAMES structure is the cetane number, a measure of the fuel's auto-ignition ability. The longer the fatty acids chain length and saturation, the higher is this number and better is the ignition quality [55]. This number is obtained by the standard number of 100 for cetane hydrocarbon, that easily ignites under pressure. Comparing to conventional diesel fuels, biodiesel has a higher cetane number (more efficient), it is also better in flash-point, the temperature required to ignite when in contact with a spark or flame, and it is biodegradable [55][57].

In terms of supplied energy and engine performance, density property is essential and it is directly proportional to the energy content [62]; viscosity is a flow indicator that influences the operation of fuel injection equipment and its atomization. Fuels with low viscosity may compromise the engines mechanical integrity originated by leakage and power loss; on the other hand, highly viscous fuels have poorer combustion efficiency since droplets are formed in injection [55].

Some oleaginous microorganisms are rich in PUFAs, being quite different from vegetable oils. However both have favourable environmental properties, since they contain no aromatic compounds and other harmful substances. [57]. The degree of unsaturation in FAMES chemical structure, particularly the presence of double bonds, have a negative effect on the biodiesel oxidation stability, essential for distribution and storage intentions in large-scale production schemes. This explains why EN 14213 limits linolenic acid (C18:3) percentage to <12% in biodiesel content [62]. Therefore, biodiesel derived from non-conventional sources (including microbial oils) must comply with the biodiesel characterization international standards.

1.5. Cultivation systems to grow heterotrophic microalgae

There are three different modes of microalgae cultivation: continuous, fed-batch and batch mode. In the pharmaceutical industry, for example, the continuous mode is not very popular due to the high probability of contaminations and mutations [64].

Batch processes are more attractive given their robustness and simplicity, yet the only way to achieve high-cell-density is to follow a fed-batch regime, which, despite being more complex, allows the monitoring of the strains' metabolism [64]. In addition, high-cell-density cultures result in cost savings in terms of product recovery compared to low-cell-density batch cultures.

Heterotrophic cultivation systems to grow microalgae are light independent, cheaper, easier to maintain in large-scale, and are associated to higher biomass concentrations and fermentation

processes are reproducible. *C. cohnii* growth has been achieved in large scale conventional fermenters and in fed-batch regimes, obtaining high cell densities; using acetic acid as carbon source, Ratledge *et al.* performed fed-batch cultivations in 3.5 L and 5 L fermenters obtaining 20-30 g/L (DCW) biomass concentrations [27]; Swaaf *et al.* in 2 L bioreactors obtained 83 g/L (DCW) and 109 g/L (DCW) in pure ethanol and pure acetic acid feedstocks [28][34].

High-cell-density fed-batch cultivation of DHA by *C. cohnii*, also performed by De Swaaf *et al.*, on acetic acid, resulted in a high oxygen demand, which led to a large increase in stirring speed in order to maintain the aerobic conditions. The limitation in oxygen turns out to be one of the major disadvantages of using fed-batch on a commercial scale, as well as the problems resulting from the increase in heat from power input in mixing, which can culminate in cooling issues [34][64].

1.6. Flow cytometry

Microalgal culture monitoring by Flow Cytometry (FC) is an effective technique that provides information on cells physiological states, instead of the traditional methods to monitor culture developments, such as DCW, optical density and cell counting [21]. This is especially important when cells are growing in media containing industrial wastes, since this condition may reduce the process performance due to the presence of inhibitory compounds that affect cells metabolism [15][18].

At-line multi-parameter cytometry combined with specific dyes allows the control of bioprocesses, leading to an efficiency optimization. The understanding of cell survival mechanisms on stress situations, cell functions and compartments improves cultivation evolution, since it is possible to change operational conditions and enhance metabolic engineering near real time [15][19].

Figure 1.7 represents cell target sites, as well as some commonly stains which are used in association with FC, to detect cell functions and products. Some dyes accumulate in cell compartments selectively or trigger their properties modifications, via biochemical reactions, such as enzymatic activity, intracellular pH, membrane integrity, respiratory activity, and membrane polarization, as an attempt to overcome environmental changes. Others have the capacity to bind specifically to cell components or molecules (lipids, proteins and nucleic acids) [66].

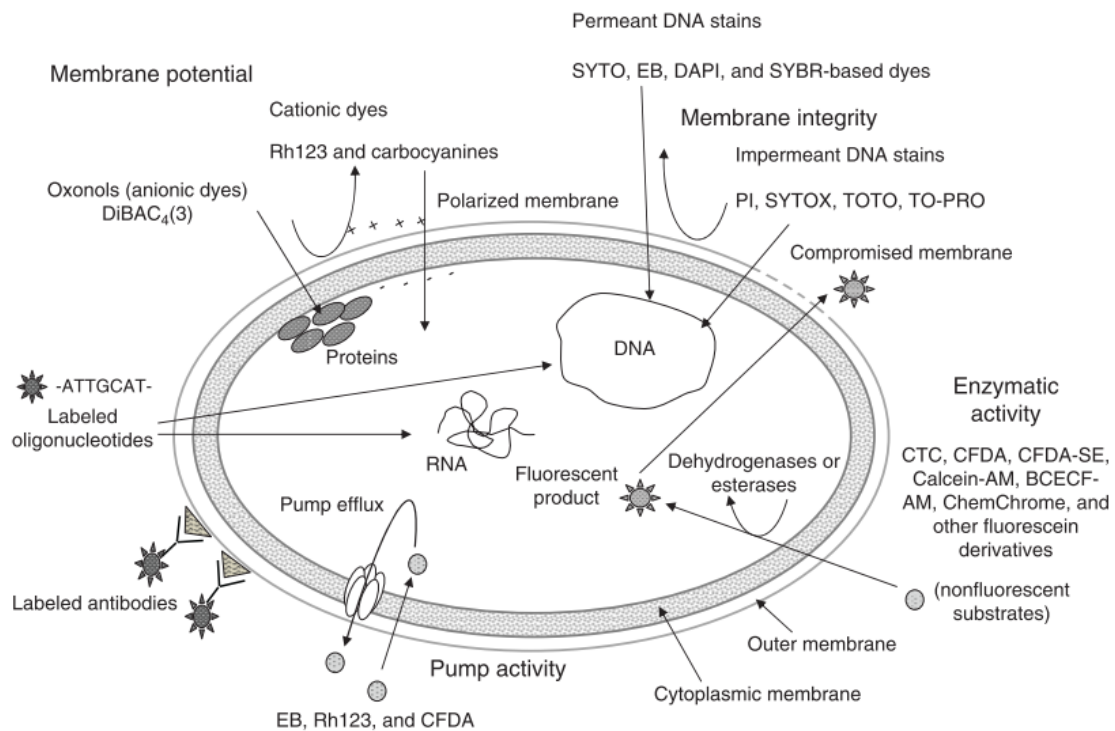


Figure 1.7 - Schematic representation of different cell target sites and variety of stains for fluorescent labelling used in combination with FC [67].

Moreover, as microalgae are large unicellular microorganisms, they are ideal for FC analysis, being clearly distinguished from the background and noise [21]. De Jara *et al.* [68] used FC combined with Nile Red (fluorescent dye) to quantify *in vivo* *C. cohnii* lipid and DHA production.

In this study FC was used to monitor *C. cohnii* cell physiological response (membrane integrity and enzymatic activity), as high percentage of injured or dead cells present in the cultivation will reduce the process efficiency; additionally, cell counting was performed as a measure of *C. cohnii* biomass concentration.

1.6.1. Equipment

FC technology characterizes cell populations, at single-cell level, as they flow in a fluid stream and are illuminated by a laser beam. The intensity of the optical signals produced, from scattering or fluorescence (when dyes are used) are correlated with multiple physical properties of single particles, including their relative size and internal complexity [21][23].

A common FC equipment is composed of a few components: a light source, optical filters with different wavelengths, the hydraulic fluidics system (flow cell), photomultiplier tubes or a group of photodiodes to detect the signals of interest and, finally, a data acquisition and processing unit [67] (Figure 1.8).

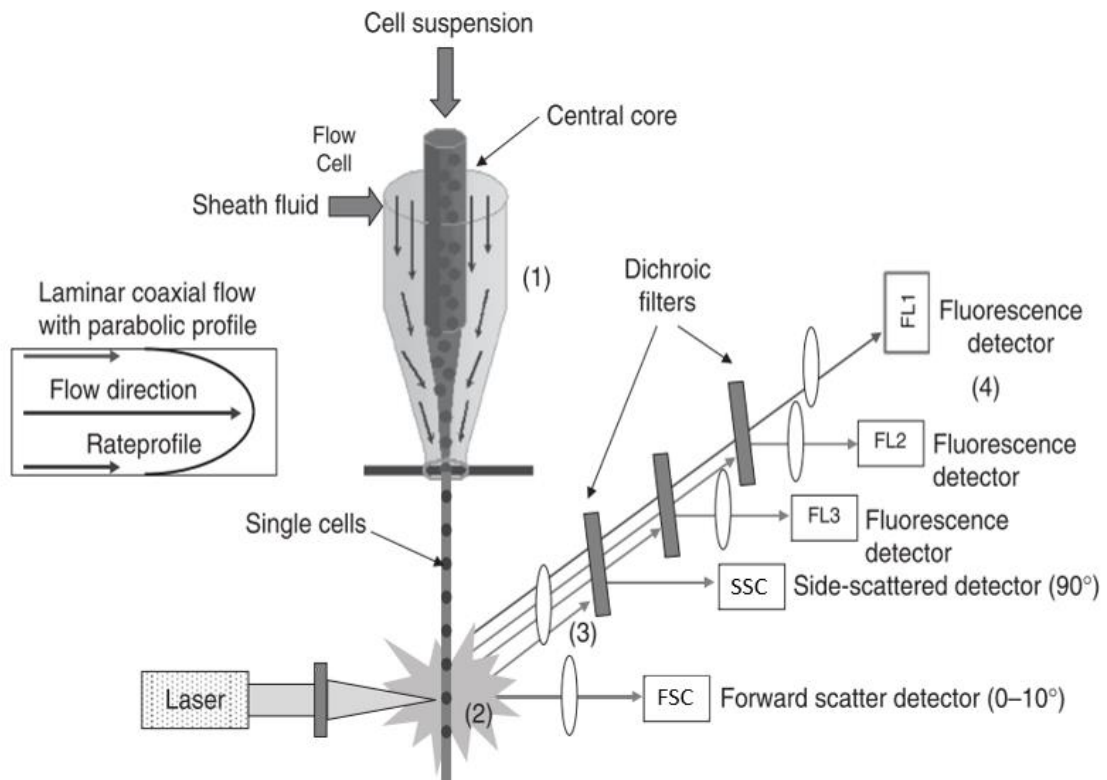


Figure 1.8 - Typical flow cytometer schematic representation: The hydraulic fluidics system allows the formation of single cell stream in the flow cell (1). When cells pass through a laser beam and contact with the laser in a restricted position, different signals are emitted concerning to multiple cell parameters (2). According to certain wavelengths, scattered and fluorescence emissions of each particle are separated by mirrors (optical system) and a group of filters (3). A detection system can collect the signals formed by a collection of photodiodes, two scattering (FSC and SSC) and three fluorescence (FL1, FL2, and FL3) detectors, in this case (4). Lastly, signals are sent to a computer, obtaining a data visualization of the population regarding different parameters. Reproduced from Diaz *et al.* [67].

The fluidics system is responsible of transporting particles in a high-speed fluid stream (up to 100 cells/s). When cells are intercepted by one or multiple laser beams, fluorescent molecules are excited and the scattering properties are measured [66]. There are two types of scattering: (a) forward scatter (FSC), measured in the plane of the beam (0-10°) and gives information on cell size; (b) side scatter (SSC), measured at 90° to the laser beam, which provides information concerning cell internal features [66].

For each particle, the scattering signals are unique and can be distinguished in heterogenous samples of different cell types (and debris). Data acquisition is the graphic visualization of scattering, and fluorescence cell parameters are converted into density plots having the relative contribution of different regions. In Figure 1.9, each single cell is designed as an *event*, and settling *gates* (R-1, in blue, Figure 1.9, a)) allows the selection of the studied cell population.

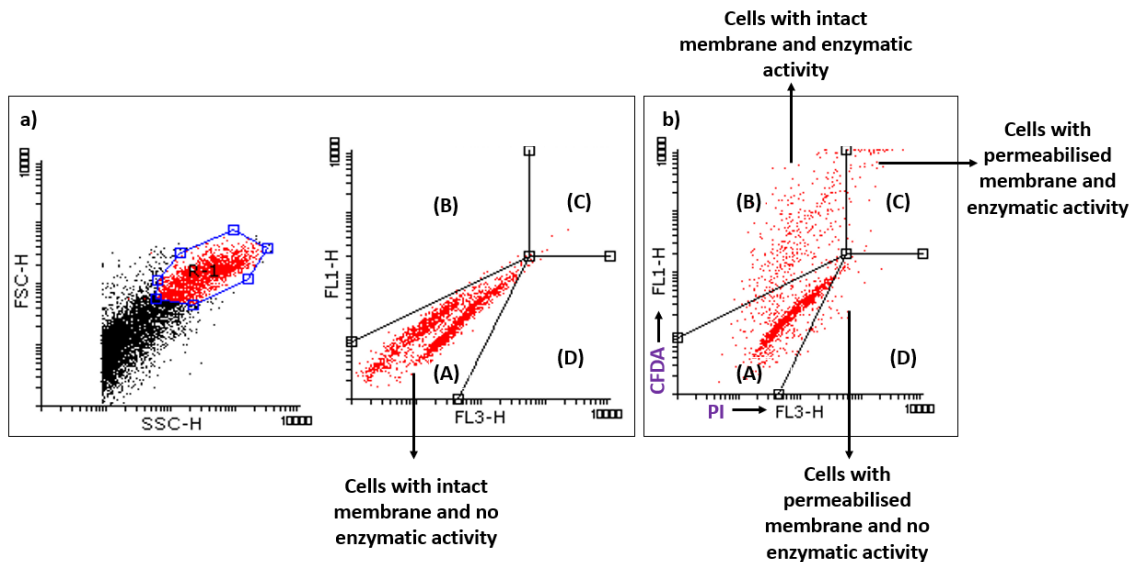


Figure 1.9 - FC controls for population identification ((A), (B), (C) and (D)). a) Density plots for autofluorescence; and b) Density plot for cells stained with Carboxyfluorescein diacetate and Propidium iodide mixtures in FL1 and FL3 detectors.

In the present work two flow cytometer equipment were used, FACSCalibur™ from Becton Dickinson (USA) and CytoFLEX from Beckman Coulter Life Sciences (USA).

FACSCalibur™ equipment was initially used. It is composed of two light sources, blue argon (488 nm) and red diode (635 nm), with FSC and SSC detectors working at the same wavelength as blue argon laser. Regarding fluorescent detectors, all sensitive in visible spectrum: FL1 in green region (530 nm ± 30 nm), FL2 in yellow region (585 ± 42 nm), FL3 in orange region (> 670 nm), and an additional photomultiplier FL4 in red region (600 ± 16 nm).

In the middle of the experimental work, the FACSCalibur™ FC was replaced by a CytoFLEX FC equipment, comprised 3 standard wavelengths lasers: blue (488 nm), red (638 nm) and violet (405 nm). Each Wavelength Division Multiplexer (WDM) corresponds to a different laser (or in some cases two lasers) and 13 band pass filters can be replaced inside as needed (Figure 1.10). FITC corresponds to FL1, PE to FL2 and PC5.5 to FL3.

















Lasers	Fluorescent Channel	CytoFLEX Channel Names	Commonly used Fluorescent Dyes
 488 nm	 525/40 BP	FITC	FITC, Alexa Fluor™ 488, CFSE, Fluo-3
	 585/42 BP	PE	PE, PI
	 610/20 BP	ECD	ECD, PE-Texas Red®, PE-CF594, PI
	 690/50 BP	PC5.5	PC5.5, PC5, PerCP, PerCP-Cy5.5, PI, DRAQ7™
	 780/60 BP	PC7	PC7, DRAQ7™
 638 nm	 660/10 BP	APC	APC, Alexa Fluor™ 647, eFluor™ 660, Cy5
	 712/25 BP	APC-A700	APC-A700, Alexa Fluor™ 700, Cy5.5, DRAQ7™
	 780/60 BP	APC-A750	APC-A750, APC-Cy7, APC-H7, APC- eFluor™ 780, DRAQ7™
 405 nm	 450/45 BP	PB450	Pacific Blue™ dye, V450, eFluor™ 450, BV421
	 525/40 BP	KO525	Krome Orange, AmCyan, V500, BV510
	 610/20 BP	Violet610	BV605, Qdot® 605
	 660/10 BP	Violet660	BV650, Qdot® 655
	 780/60 BP	Violet780	BV785, Qdot® 800

Figure 1.10 - CytoFLEX (Beckman Coulter Life Sciences, USA) WDM Optical Filter Display Colour Codes, channel bandpass (BP) filters names and commonly used fluorescent dyes [70].

Some FC detection problems may arise when more than one dye is applied simultaneously, despite the fact that fluorescent dyes have a wide emission spectrum, emitted photons signal of one dye can bleed into a detection channel of another dye (spectral spillover) [71]. In multicolour flow cytometry, spillover is solved by a method referred as compensation, where FC software calculate by a linear function of the amount of the spillover fluorescence and the fluorescence intensity at the same photomultiplier and respective filter [71].

1.6.2. Enzymatic activity

The most common way to evaluate the enzymatic activity by FC is by measuring the esterase activity, using fluorescein and/or fluorescein derivatives, the last one with particular interest due to better signals quality, associated with efflux of fluorescein over time [66].

In this study, the dye carboxyfluorescein diacetate (CFDA), a non-fluorescent compound, enter the cells by passive diffusion and by the action of intracellular enzymes (esterases) it is hydrolysed to a fluorescent substance, that is retained in cells with intact membranes [67].

Therefore, if a cell is not stained with CFDA, it means that its enzymatic system is not active, or the membrane is compromised and the fluorescent product left the cell [33]. Thus, combining a dye for membrane integrity is a prerequisite to properly evaluate cell status with CFDA.

1.6.3. Membrane Integrity

Cell viability can be proved by the assessment of membrane integrity, which indicates that cells are capable of generating electrochemical gradients (membrane potential), and consequently demonstrate metabolic activity, due to active or passive transport across not damaged cytoplasmic membranes [66].

Dye exclusion methods are suitable for the detection of membrane integrity, as damaged or compromised membranes are permeable to those dyes that entering the membrane, they emit fluorescence once the linkage with some molecules is established [67]. Propidium iodide (PI) was the dye used in this study to detect cell membrane damage, since it stains cells with defective membranes by binding the cell's DNA molecules.

1.6.4. Flow cytometry applications

In microalgal biotechnology FC coupled with fluorescence-activated cell sorting (FACS) enabled the improvement of sophisticated high-throughput methodologies, not only to obtain products of interest, but also in CO₂ mitigation process and bioremediation of effluents [72]. Taborda *et al.* [33] used FC combined with CFDA and PI fluorescent stains to monitor *C. cohnii* physiological states during the microalgal cultivations on different substrates.

Concerning aquatic microbiology, a straightforward total single-cell counts growing (colony forming units – CFUs) to the analysis of entire communities structures by FC, that when combined with genomics and proteomics for research purposes facilitate the management and monitoring of those communities in field biosafety investigation and drinking water treatment procedures [73]. Thus, FC data is applied in the prediction of more precise kinetic models in bioprocess engineering, by parameters monitorization over time obtaining detailed kinetic profiles of cell growth, substrate consumption and/or product formation [67]. Bioprocess designs rely on a real view of events occurring inside the bioreactor based on improved kinetic model that take into account cell heterogeneity, besides the contribution of single subpopulations in different stages [67]. Díaz *et al.* developed a segregated kinetic model, considering both viable and dead cells, to describe batch cultures of *Lactobacillus hilgardii* and *Saccharomyces cerevisiae*, achieving a real time deep understanding of populations dynamics, that allow investigation of different strategies to increase the overall process efficiency [74].

Regarding microalgae cultivation monitorization by FC, Satpati and Pal [75] using Nile red stain, developed a protocol for the rapid detection of neutral lipid production in situ in the green microalgae *Chlorella ellipsoidea* and *Chlorococcum infusionum*. Chioccioli *et al.* [76] estimated the biomass dry weight in the microalgae *Chlamydomonas reinhardtii* and *Chlorella vulgaris* with FC pulse width data. Finally, there were several investigations to the marine dinoflagellate microalgae *C. cohnii*, Lopes *et al.* [65] used multi-parameter FC to study the impact of n-dodecane additions in batch fermentations.

1.7. Objectives

The main objective of this work was to establish a protocol to optimise *C. cohnii* ATCC 30772 biomass and lipid production, using a 7 L benchtop bioreactor, operating under fed-batch mode, and using crude glycerol as carbon source.

Flow cytometry was used to monitor, in real time, cellular parameters such as biomass growth and cell viability to evaluate the microalgae cell physiological response to the growth conditions. The cultures were also monitored in terms of dissolved oxygen percentage (DO), carbon and residual nitrogen concentration, fatty acid content and DHA content. Correlations were established between DCW, optical density, and cell number.

The fatty acids composition in the saponifiable fraction of *C. cohnii* lipids was analysed, to evaluate its potential as DHA and biodiesel source, following the European standard for this product.

2. Materials and Methods

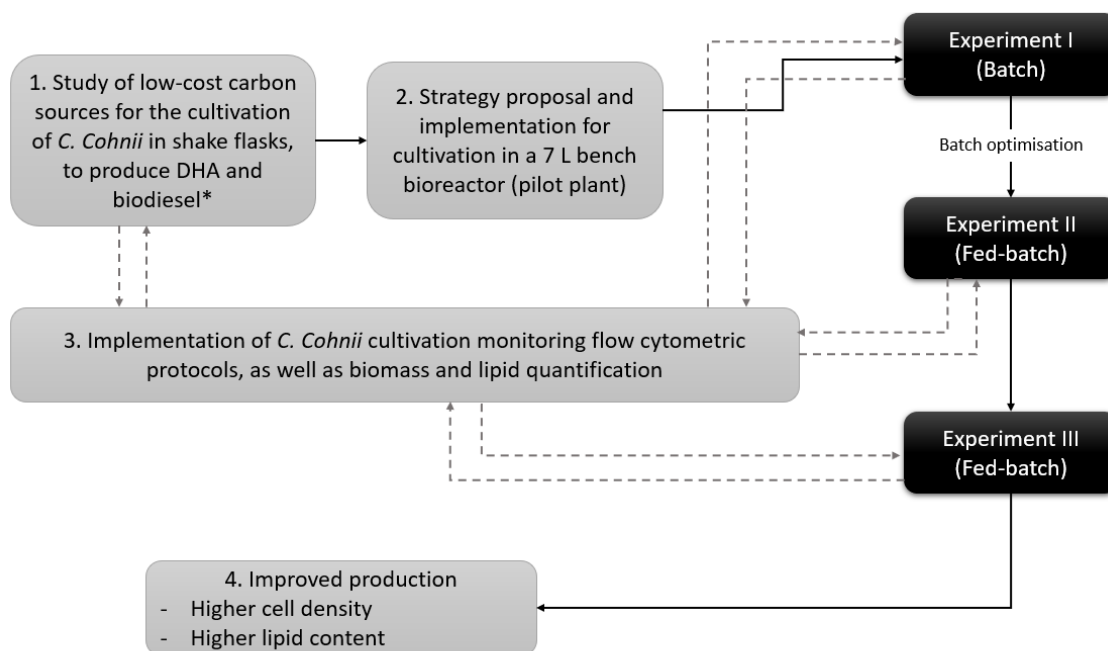
2.1. Reagents and Equipment

Table A.1 (Appendix A) lists all the chemicals used during this experimental work. Equipment used will be referred when used along this text.

2.2. Experimental strategy

All the experiments were performed in a 7 L bench bioreactor, in batch and fed-batch modes of operation, to obtain high cell density cultures of the marine microalgae *C. cohnii*.

Based on a previous study concerning low-cost carbon sources for the cultivation of *C. cohnii* in shake flasks reported by Taborda et. al, 2021 [33], the chosen carbon source for further experiments was crude glycerol, a by-product of biodiesel industry. Figure 2.1 summarizes the experimental strategy (steps 2 and 3), as well as the main objectives (step 4).



*Taborda et al. 2021

Figure 2.1 - Experimental strategy development (experiments I, II and III) carried out during the present work.

Experiment I was conducted in batch mode, to study the microalgae growth and lag, exponential and stationary phases duration. Subsequently, based on experiment I achievements and insights, the protocol was extended to fed-batch cultivations (experiments II and III).

All the 7 L bioreactor assays were carried at pH 6.5, and temperature of 27 °C. The speed rate was adjusted whenever necessary, according to the dissolved oxygen percentage (DO, %) in the medium, to avoid oxygen limiting conditions, usually present in high *C. cohnii* cell dense suspensions [34].

Experiment II was carried out in fed-batch mode, to achieve higher microalgal biomass and lipid concentrations, since the exponential growth phase is extended by the addition of a nutrient concentrated solution. However, high residual glycerol concentrations were detected in the broth, which could have inhibited the microalgal growth and lipid synthesis. Therefore, experiment III was carried out to reduce the nutrient concentrations in medium, using a nutrient concentration solution with half of the nutrient concentration used in experiment II, to avoid growth and lipid synthesis inhibition by substrate. Moreover, during this assay, the biomass concentration was assessed by flow cytometry (as cell number/mL) which was correlated with DCW. This strategy improved the biomass determination accuracy during the microalgae cultivations, since the growth medium containing crude glycerol and corn steep liquor, which contained many particles which interfered in the biomass quantification.

2.3. Strain and Starter Cultures

In this study *Cryptocodinium cohnii* (ATCC 30772) cells were maintained as static cultures (150 mL in 250 mL shake flasks) on a standard medium composed of sea salt (23 g/L) and yeast extract (1.8 g/L) and a carbon source (9 g/L), at 25 °C in the dark. Glucose and glycerol were the two carbon sources used. All medium components were heat sterilised (Uniclave 88, Portugal or A. J. Costa LDA., Portugal) at 121 °C for 20 min, apart from glucose, to avoid its caramelisation (Maillard reaction). Also, to prevent bacterial medium contaminations, a filtered solution (0.2 µm) containing three antibiotics (the solution of antibiotics contained chloramphenicol (5 mg/L), penicillin G (62 mg/L) and streptomycin (100 mg/L)), were added to the sterilised medium.

These cultures were re-inoculated in the same medium monthly and were used to as seed for further experiments.

2.4. Carbon source

Crude glycerol (previously distilled), a by-product of biodiesel industry, was the carbon source used in inoculum cultures and the media culture of the bioreactor experiments (I, II, III).

Previously the composition of the crude glycerol, kindly supplied by Iberol (Alhandra, Portugal), was analysed ([77]) and is presented in Table 2.1.

Table 2.1 - Composition of the crude glycerol supplied by Iberol (Alhandra, Portugal), used in experiments I and II [77].

Component	Percentage (w/w%)
Glycerol	83.2
Water	11.2
Methanol	0.013
Non-glycerol organic matter (NGOM)	0.89
Ashes	4.74
Sodium	1.04
Potassium	<0.0005

For experiment III, the crude glycerol was similarly analysed since it was a new supply from Iberol. The compositions obtained are listed in Table 2.2.

Table 2.2 - Composition of the crude glycerol supplied by Iberol (Alhandra, Portugal), used in experiment III.

Component	Percentage (w/w%)	Assay method
Glycerol	83.8	Ea 6-51 (AOCS)
Water	9.90	EN ISO 12937
Methanol	0.007	LBB internal method*
Non-glycerol organic matter (NGOM)	n.d	NF T 60-368
Ashes	6.54	NP 1688

n.d – non-detectable

* - Reference method: EN 14110/2003

The non-glycerol organic matter (NGOM) was not detected, since its determination is based on glycerol, water, and ashes content (which total sum is 100.24%). This is expected since glycerol, water and ashes content determination were determined by different methods.

2.5. Inoculum

The inocula for the 7 L bioreactor experiment were prepared in shake-flask cultures (500 mL flasks, at 150 rpm) containing 135 mL of medium and 10% v/v of the starter culture (15 mL). The medium for these cultures contained yeast extract (0.5 g/L), crude glycerol (23.94 g/L, in order to obtain 20 g/L of glycerol in the medium), corn steep liquor (CSL, 4.59 g/L) and sea salt (25 g/L). The pH was adjusted to 6.5 using NaOH (5 mM) and HCl (5 mM), and all media were autoclaved (Uniclave 88, Portugal) at 121 °C for 20 min.

The pH determination was performed using a Mettler probe and a Consort C3021 potentiometer (Consort, Belgium), calibrated regularly.

1 mL of the antibiotic solution (Section 2.3) was added to the inocula (1 mL/L), and culture media used in the 7 L bioreactor. The inocula were grown for 6-7 days, in an agitated incubator (Unitrom Infors, Switzerland) in the dark, at 27 °C and 150 rpm.

2.6. Cultivation in bioreactor

Experimental assays (I, II and III) were carried out in a 7 L bioreactor, with 5 L of working volume (FerMac 310 bioreactor, Electrolab Biotech, United Kingdom), coupled with a controller module composed by a stirrer, dissolved oxygen, temperature, pH probes, and foam formation sensor (FerMac 360 bioreactor, Electrolab Biotech, United Kingdom). Before inoculation, the bioreactor, with the culture media was sterilized in the autoclave (Uniclave 88, Portugal or A. J. Costa LDA., Portugal), at 121 °C, for 30 min.

Under asepsis conditions, 297 mL of the inoculum, and 3 mL of the antibiotic solution were added to 2700 ml of culture medium (same as inoculum), making up the total volume of 3000 mL.

By automatic addition of 2.5 M NaOH or 2.5 M HCl, the pH was regulated to the pH set-point (6.5). The anti-foaming agent, polypropylene glycol, was manually added whenever necessary, in a 1:10 concentration. Mixing was assured by a Rushton turbine, the heating with a jacket and four baffles were introduced to improve the mass transfer rate.

At the beginning of each assay, the oxygen probe (Broadley James, USA) and pH electrode (Mettler Toledo™ 405-DPAS-SC-K8S/325, USA) were calibrated according to the manufacturer's instructions.

DO in the medium was controlled by the stirring and aeration rates, assuring that the microalgae growth was not limited by oxygen. Initially the speed rate was set at 300 rpm, and was adjusted according to DO readings (kept above 30% of air saturation); the temperature set-point was 27 °C.

During all *C. cohnii* cultivations, samples were collected under asepsis conditions for optical microscope observation, biomass (DCW and OD), residual glycerol and nitrogen determinations, and flow cytometry analysis.

The samples collected (10 mL) were centrifuged (Sigma 2-16K, Sartorius, Germany) in falcon tubes during 10 min, at 7000 rpm and 4 °C. The supernatant was kept in another falcon tube, and the pellet (biomass) was stored in a freezer (-18 °C). Afterwards, the supernatant was analysed for total nitrogen (Kjeldahl method) and residual glycerol concentration (High-performance liquid chromatography, HPLC); biomass pellet was lyophilized (Heto PowerDry LL3000 Freeze Dryer, Thermo Scientific, USA) for 48 h and further analysed for fatty acid content determination. For each sample, the ashes, organic matter, and moisture contents were also determined.

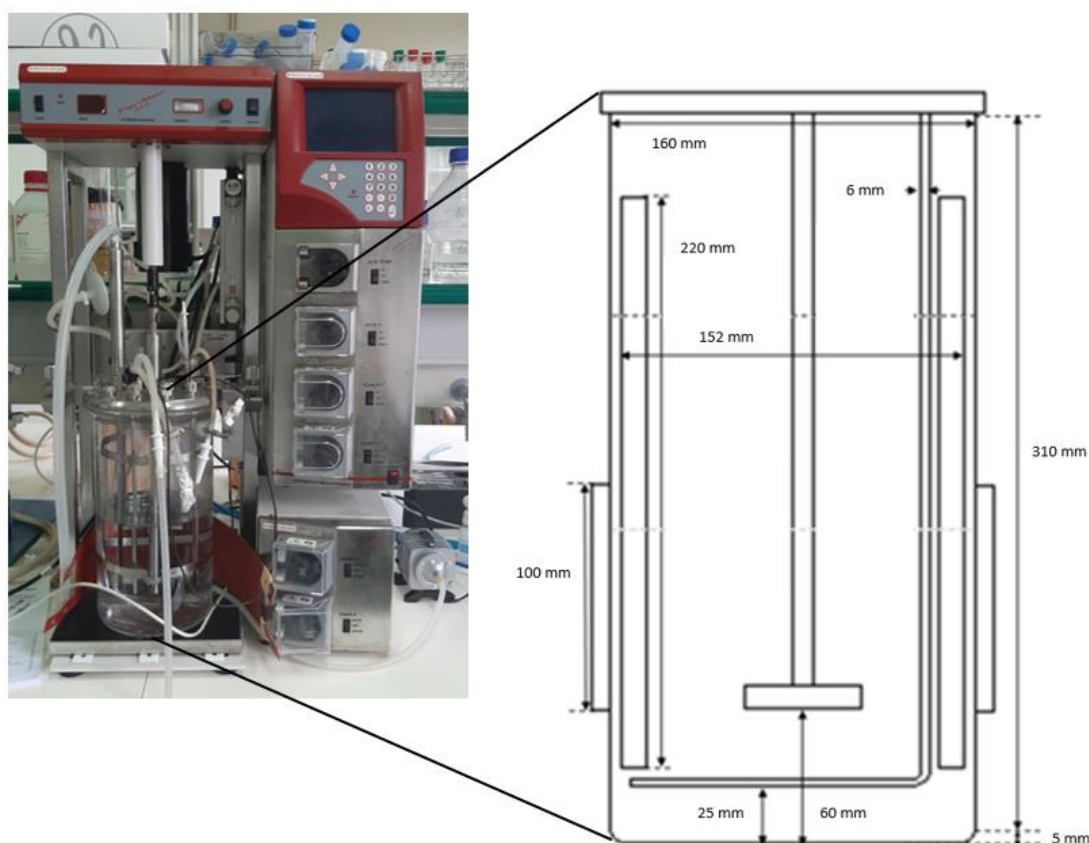


Figure 2.2 - Bioreactor and controller module used in the experiment (left); schematic representation with main bioreactor dimensions (right) [78].

The experiment I was carried out as a preliminary assay to study *C. cohnii* batch growth in culture medium containing crude glycerol and corn steep liquor; afterwards *C. cohnii* was grown in a 7 L bioreactor under fed-batch mode (assays II and III). At the end of the exponential phase, the bioreactor was fed a 5 times concentrated nutrient solution in experiment II and 2.5 times concentrated in experiment III, that was pumped using a peristaltic pump (Watson Marlow 520 Du, United Kingdom), adjusting the feeding rate according to DO readings, biomass and residual glycerol concentrations.

2.7. Analysis of biomass concentration

For experiments I and II, the two methods used to quantify the biomass concentration were optical density (OD) readings, and DCW determination. A previous correlation between OD and DCW was established.

To measure the DCW, 1 mL of sample duplicates were collected in Eppendorfs (1.5 mL) previously dried in a 100 °C oven (Mettler, Germany) for 18h, following 30 min cooling, in a low humidity atmosphere of a desiccator, and weighted. After samples centrifugation (Beckman Avanti J-25I, EUA), at 5 min, 7000 rpm and 20 °C, the pellet was washed once with distilled water to remove the medium salt. Afterwards, the biomass pellets were placed in the oven, at 100 °C for 24h, cooled and weighed.

In experiment III, the biomass concentration was evaluated by cell number/volume assessed by flow cytometry, in triplicate, in order to eliminate the interference of the particles present in the growth medium due to the corn steep liquor (CLS) and crude glycerol presence. A previous correlation between the cell number/volume and DCW, and cell number/volume and OD was established (Section 3).

To all samples taken throughout the experiment, their OD was discounted by the OD and the dry weight of the cell-free medium, with pre-washed cell pellet.

2.8. Flow Cytometry

This study used two different flow cytometers to monitor *C. cohnii* cell physiological status throughout assays, as well to quantify the biomass:

Experiment I and II were carried out using a BD FACScalibur™ cytometer (Becton Dickinson, Franklin Lakes, NJ, USA), equipped with an argon laser and a red diode laser which radiation emission is 488 nm and 635 nm, respectively; this equipment contained, in addition, photomultipliers as fluorescence detectors - FL1 (green: 530 ± 30 nm), FL2 (yellow: 585 ± 42 nm), FL3 (orange: > 670 nm) and FL4 (red: 600 ± 16 nm) [79], that from stained samples with CFDA and PI, cell enzymatic activity and cell membrane integrity was examined using Flowing Software 2.5.0 tools.

For experiment III, a CytoFLEX flow cytometer (Beckman Coulter Life Sciences, USA) was used, with five channels from the 488 nm (blue) laser, three from the 638 nm (red) laser, five from the 405 nm (violet) laser. The instrument includes 13 band pass filters which can be repositioned as needed [80], the photomultipliers used in the study were FSC-A and SSC-A for auto-fluorescence; FITC-A and PC5.5-A for CFDA and PI dyed samples, respectively. Data was analysed CytExpert 2.4 software (Perttu Terho). Previous flow cytometric controls were carried out using *C. cohnii* cells at different growth conditions, to evaluate the efficiency of the flow

cytometric protocol in association with the CFDA/PI mixture, to identify different cell physiological status. These controls were then compared with data obtained during the microalgal cultivations [77].

All culture samples were sonicated (Transsonic T 660/H, Elma, Germany) for 10 s, at 35 kHz, to remove cell aggregates, and ensure individual cell analysis.

Samples were diluted in McIlvaine buffer (pH 4.0) previously filtered in a 0.2 μm membrane (TPP Syringe filter 22, Switzerland), to remove the particles in suspension.

For *C. cohnii* enzymatic activity and membrane integrity detection, 3 μL of CFDA (10 mg/mL stock solution) and 2 μL (1 mg/mL stock solution) were added to 500 μL cell suspension, incubated for 15 min in the darkness. Before cell analysis, the sample was always mixed in the vortex to avoid cell deposition in tube bottom.

2.9. Microscopic Observations

To verify possible contaminations, all samples collected from the bioreactor were observed, as well as the starter and pre-inoculum cultures before bioreactor inoculation. The observations were performed under visible light using the Olympus BX60 fluorescence microscope (Olympus Corporation, Japan), with mercury fluorescence illuminator and Nomarski/DIC Prism for transmitted light [81].

2.10. Nitrogen source and total nitrogen amount determination

The total nitrogen concentration in the sample supernatant were quantified according to the modified Kjeldahl method adapted from the standard 4500-N_{org} [82].

This determination was also carried out for nitrogen content quantification in the corn steep liquor (CSL), a nutrient used in the medium formulation as nitrogen source, to define the appropriate amount to add to the growth medium. CSL was graciously supplied by COPAM, Companhia Portuguesa de Amidos SA, S. João da Talha, Portugal. After collected from the industrial plant, the CSL was left uncovered, for a few weeks, so that volatile toxic compounds could be released. This substrate contains 0.035 g nitrogen/g.

0.5 g of CSL, and 5 mL of samples were transferred to the digestion tube, in duplicate; 20 mL of concentrated sulphuric acid (96%), and 1 g of a catalytic mixture (30 g of copper, 30 g of titanium oxide, 10 g of stearic acid and 930 g of potassium sulphate), were added to the tubes, to convert the nitrogen present in the organic matter into ammonium sulphate. The tubes were then

placed in the digestion equipment (Tecator Lab Digestion System 6, 1007 Digester, Switzerland), being heated to promote the reaction for 2 hours.

Once completed the digestion, the tubes were cooled at room temperature. In a 150 mL Erlenmeyer tube, 50 mL of boric acid and two droplets of pH indicator (2 g methyl red and 1 g methylene blue, dissolved in 100 cm³ of 95% (v/v) ethyl alcohol) were added. These Erlenmeyer tubes, paired with digestion tubes, were positioned in the distillation unit (Tecator Kjelttec System 1026 Distilling Unit, Switzerland), which introduced distilled 50 mL water and 100 mL NaOH solution 50%, which causes the release of ammonia that is steam distilled and collected in a dilute boric acid solution.

The ammonia was quantified by titration with hydrochloric acid (0.1 N) which, in the presence of the pH indicator, changes from light blue to dark blue at pH 5.4.

The total nitrogen content of each sample, as a percentage, was calculated using (1). V is the HCl (0.1 N) volume in mL spent in the sample titration, and m is the mass, in grams, of the tested sample.

$$\text{Nitrogen (\%)} = \frac{0,14 \times V \text{ (mL)}}{m \text{ (g)}} \quad (1)$$

2.11. Ash and moisture content determination

Moisture and ash content of biomass samples was sequentially determined, to further correct the biomass weight used for FA analysis.

100 mg of lyophilized sample were accurately weighed (triplicate samples) in previously weighed calcined crucibles, which were placed in an oven at 100 °C for 24 h; thereafter, the crucibles containing the biomass were cooled in a desiccator and weighed. The moisture content was calculated according to (2).

$$\text{Moisture (\%)} = \frac{m_{\text{crucible+biomass}^*} - m_{\text{empty crucible}^*}}{m_{\text{biomass}}} \times 100 \quad (2)$$

*mass after oven 100 °C.

Afterwards, the crucibles were placed in a muffle furnace at 550°C for 1 h, cooled in a desiccator and weighed to determine the ash content (3).

$$\text{Ash(\%)} = \frac{m_{\text{crucible+ash}} - m_{\text{empty crucible}}}{m_{\text{biomass}}} \times 100 \quad (3)$$

2.12. Identification and quantification of lipids as total fatty acids (TFA)

Gas chromatography (GC) was used to determine *C. cohnii* lipid content and fatty acid profiles.

To achieve that, a transesterification reaction was applied to *C. cohnii* freeze-dried biomass to transform the mono-, di- or triglycerides into the respective FAMES. The procedure protocol used was an adaptation of the described by Lepage and Roy (1986) [65].

In test tubes approximately 100 mg of lyophilized biomass samples (Heto PowerDry LL3000 Freeze Dryer, Thermo Scientific, USA, with a vacuum pump - vacuubrand, Germany) reacted with 2 mL of a mixture of methanol/acetyl chloride (95:5 v/v), prepared beforehand in a cooling bath due to the exothermic reaction nature. Heptadecanoic acid (C:17, 5 mg/mL, Nu-Check-Prep, Elysian, USA) was added as internal standard to the tubes (0.2 mL).

The tubes were sealed under nitrogen atmosphere (to avoid sample oxidation) and the reaction occurred for 1 hour, at 80 °C, in the dark. After cooling down to room temperature, 2 mL of n-heptane were added for the extraction of the methyl esters and 1 mL of distilled water to promote phase separation. The heptanoic phase (upper phase) was filtered using a glass Pasteur pipette and a cotton filter with a bed of anhydrous sodium sulphate and collected in glass vials also under nitrogen atmosphere.

The samples were analysed in a gas-liquid chromatograph (SCION GC 436 from Bruker, Germany), equipped with a flame ionization detector (FID). The separation of the compounds was performed on a fused silica capillary column (Supelcowax 10, SUPELCO, USA), 30 m long, 0.32 mm internal diameter and 0.25 µm film thickness. Helium was used as carrier gas at a flow rate of 1.6 mL/min.

The initial column temperature was set at 200°C for 20 min at a heating rate of 2°C/min until a final temperature of 220°C was reached, with a column pressure of 13.5 psi. The injector and detector had a temperature of 250°C and 280°C, respectively, and the split ratio was 1:20 for 5 min, then 1:10 for the remaining time.

Each sample was processed in duplicate, and each duplicate was injected once.

The FAMES were identified by comparison with the retention times of the components of standard 461 (Nu-Chek-Prep, Elysian, MN, USA). The quantification of each of the fatty acids was performed according to (4), where m_{FA_i} is the mass of fatty acid i , A_{FA_i} is the area of the fatty acid peak, $A_{(17:0)}$ is the area of the peak corresponding to the internal standard and RF_{FA} is the response factor of the fatty acid FA_i .

$$m_{FA_i} = \frac{A_{FA_i}}{A_{(17:0)}} \times RF_{FA} \quad (4)$$

2.13. HPLC

To determine the glycerol content, samples were filtered and injected (LaChrom L-7200 (Hitachi, Japan) in a HPLC column, Aminex™ HPX-87P (Bio-Rad, California, USA). This Agilent Chromatographer was equipped with a diode array detector (DAD) and a refractive index detector (RI).

The software used to analyse the chromatograms was the Chromeleon™ Chromatography Data System (CDS) software. (ThermoFisher Scientific™, USA).

2.14. Kinetic parameters determination

2.14.1. Reaction rate

The rate of chemical reactions is defined as the variation of a substance *i* concentration over the reaction time, i.e., the slope of concentration of *i* throughout time (r_i). By (5), r_i can be calculated and ΔC_i is the concentration variation in the Δt , which is the time interval corresponding to C_i variation.

$$r_i = \frac{\Delta C_i}{\Delta t} \quad (5)$$

Considering the substance *i* the total glycerol consumed, the carbon source, in the medium at time *t* of reaction, using Equation (5) is determined the volumetric substrate uptake rate (r_s). For a ΔC_i variation, between $t = 0$ and *t*, the residue of glycerol in medium is obtained for any time *t*.

Similarly, for the biomass growth (DCW) and fatty acids / DHA, the rates of formation can be obtained (r_x , r_{FA} and r_{DHA} , respectively).

2.14.2. Specific growth rate

The specific growth rate (μ_{max}) is the rate of biomass growth per unit of biomass concentration and is calculated during the exponential phase, in which the cell growth is exponential. Using (6) the specific growth rate is obtained, and DCW_0 is the dry cell weight in the moment of the inoculation:

$$\ln(DCW) = \mu_{max}t + \ln(DCW_0) \quad (6)$$

2.14.3. Average volumetric productivity

The average volumetric productivity of A in a time t ($P_{A\text{ average}}(t)$) can be determined (7) where C_A is the concentration of A at time t ($C_A(t)$) and at t_0 ($C_A(t_0)$), the initial time ($t = 0$). For each experiment, this equation was used to calculate the biomass, total fatty acids and DHA productivity (P_X , P_{FA} and P_{DHA} , respectively).

$$P_{A\text{ average}}(t) = \frac{C_A(t) - C_A(t_0)}{t - t_0} \quad (7)$$

The same equation is used to calculate the instantaneous productivity, for the time interval t considered, with $P_{A\text{ max}}$ as the maximum instantaneous productivity.

2.14.4. Fatty acid composition

The percentage of each fatty acid in the total mass of fatty acids %TFA_i (w_{FA}/w_{TFA}) is calculated by (8). % FA_i (w_{FA}/w_{TFA}) is the percentage of fatty acid i, m FA_i is the mass of fatty acid i and m TFA is the total mass of fatty acids.

$$\%FA_i (w_{FA}/w_{TFA}) = \frac{m FA_i}{m TFA} \times 100 \quad (8)$$

C. cohnii lipid content, determined as TFA, was calculated according to the following (9):

$$\%TFA (w_{TFA}/w_{\text{biomass}}) = \frac{m TFA}{M} \quad (9)$$

The total fatty acid productivity (P_{FA}) is also calculated using (10), P_X is the average volumetric biomass productivity and %TFA ($w_{TFA}/w_{\text{biomass}}$) is the percentage of total fatty acids relative to biomass, this equation can also be adapted to calculate the productivity of DHA (P_{DHA}).

$$P_{FA} = P_X \times \frac{\%TFA (w_{TFA}/w_{\text{biomass}})}{100} \quad (10)$$

2.14.5. Yield

The yield between two substances A and B ($Y_{A/B}$) is a measure of B consumption efficiency to form A , i.e, the ratio between A formation rate (r_A) and B consumption rate (r_B) for the same period Δt (11).

$$Y_{A/B} = \frac{r_A}{r_B} \quad (11)$$

Considering the biomass growth (r_X) produced by substrate consumption unit (r_S), the yield ($Y_{X/S}$) measures the effectiveness of substrate conversion to biomass. In addition, the yield can be obtained considering TFA and DHA in relation to the substrate consumption ($Y_{FA/S}$ and $Y_{DHA/S}$, respectively).

2.15. Physical parameters of biodiesel fraction determination

2.15.1. Density

Pratas *et al.* tested the predictive ability of several models for biodiesel density determination and developed an adaptation of the GCVOL predictive model, group contribution method [83]. In this study, the revised GCVOL model will be used, and it is based exclusively on the molecular structure of each component of biodiesel.

The density, ρ , is calculated by (12), in which the molecular weight, MW_j , and molar volume, V_j , are related, and x_j corresponds to the molar fraction of component j .

$$\rho = \frac{\sum_j x_j MW_j}{\sum_j x_j V_j} \quad (12)$$

(13) describes how to calculate the molar volume, V_j , of a component j ; in this equation n_i is the number of group i , and ΔV_i is the temperature dependency of the molar group in cm^3/mol , that is obtained by the polynomial function, where T is temperature in Kelvin and A_i , B_i and C_i are fixed parameters of each chemical group.

$$V_j = \sum_i n_i \Delta V_i = \sum_i n_i (A_i + B_i + C_i T^2) \quad (13)$$

2.15.2. Dynamic and Kinematic Viscosity

Based on the knowledge of a given biodiesel composition, Freitas *et al.* [84] evaluated a series of models to estimate its viscosity and proposed the revised Yuan's model, which will be used in this study, since it is the model that best describes the experimental data, corresponding to the lowest average deviation of all models tested. FAME dynamic viscosity, μ_d , is calculated by (14), that correlates the density, ρ , and kinematic viscosity, ν .

$$\nu = \frac{\mu_d}{\rho} \quad (14)$$

The density, as it is unknown, is estimated as mentioned in Section 2.15.1 Density.

By (15) the viscosity of a liquid mixture, μ_m , of n components is calculated and applied to a given biodiesel, in which x_i is the mole fraction of component i , and μ_i the viscosity of each pure FAME in mPa.s.

$$\ln \mu_m = \sum_{i=1}^n x_i \ln \mu_i \quad (15)$$

Yuan's model in (16) describes the relationship between temperature and μ_i . A , B , C and T_0 are parameters obtained by fitting real data of each pure FAME often present in biodiesel fuels, and then finally applied to the mixture model to estimate its viscosity.

$$\ln \mu_i [\text{mPa. s}] = A + \frac{B}{T [\text{K}] + T_0} \quad (16)$$

The parameters used in this study to calculate the viscosity of the biodiesel fraction obtained, by Yuan's model, are those found in the study by Freitas *et al.*, an adaptation of the model itself to their experimental data.

2.15.3. Cetane number

In 2019, Giakoumis and Sarakatsanis [85] performed an analysis of 16 predictive correlations that have been used since the early 1980s to assess the cetane number of a biodiesel, and found that the model developed by Mishra in 2016 [86], based entirely on biodiesel structural composition provides the most accurate predictions (lower average errors). In (17) cetane number, CN, can be determined, with DU as the degree of unsaturation and SCSF is the straight-chain factor.

$$CN = 63.41 - 0.073 \times DU + 0.035 \times SCSF - 3.26 \times 10^{-4} \times DU \times SCSF \quad (17)$$

DU is a measure used to take into consideration the impact of unsaturated fatty acids and is determined by (18) with w_i as the weight percentage of each FAME and n is the total number of double bonds it contains.

$$DU = 100 \left(\sum w_i^{n=1} + 2 \sum w_i^{n=2} + 3 \sum w_i^{n=3} \right) \quad (18)$$

The last metric, SCSF, is obtained by (19) with MW_i as the molecular weight of each saturated FAME.

$$SCSF = \frac{1}{100} \sum_{\text{sat}} MW_i w_i \quad (19)$$

3. Results and Discussion

3.1. Cultivations

Three cultivations of *C. cohnii* ATCC 30772 were performed according to the Section Materials and Methods. The microalgae were cultivated in a 7 L bioreactor with temperature, pH, and dissolved oxygen (DO) control. Experiment I was performed under batch mode and experiments II and III under fed-batch mode, to study *C. cohnii* growth and lipids (fatty acids) production under different operation modes.

3.1.1. Experiment I

Figure 3.1 shows the biomass concentration and productivity, natural logarithm of biomass, residual glycerol, pH, DO percentage and stirring rate profiles, for this trial. The conditions used were those considered optimal for the cultivation of *C. cohnii* ATCC 30772 mentioned in Section Materials and Methods [87].

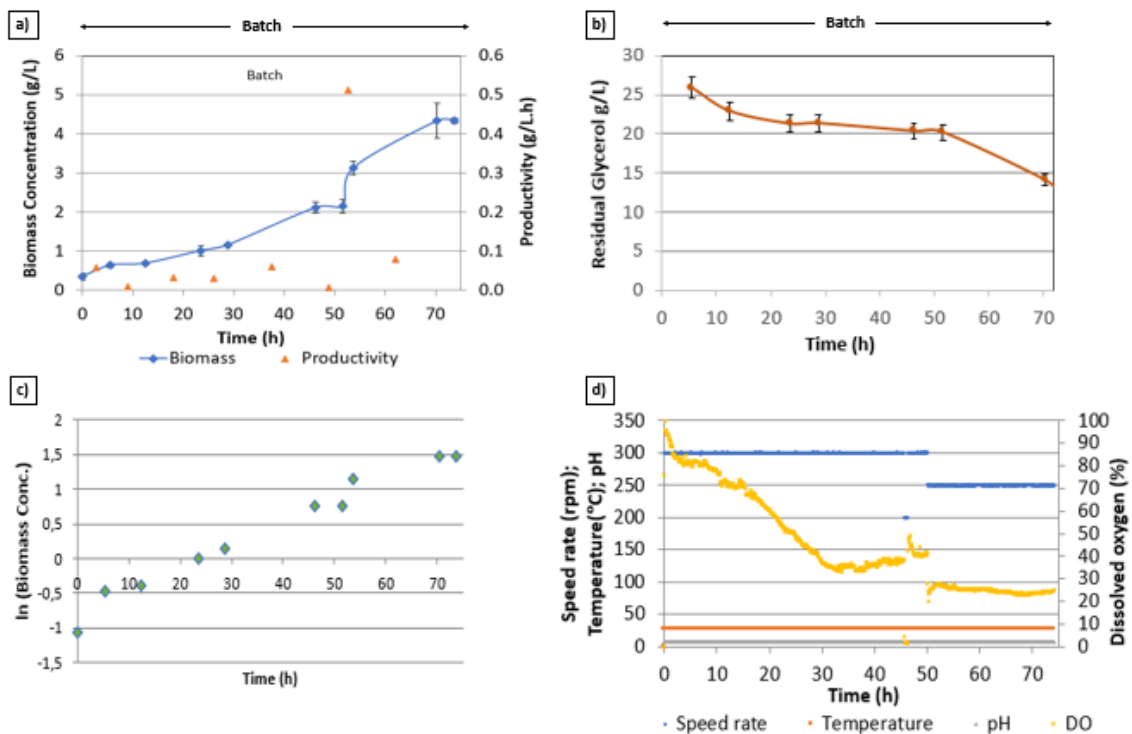


Figure 3.1 - *C. cohnii* ATCC 30772 growth in batch mode (experiment I): a) Biomass concentration and productivity. b) Residual glycerol concentration. c) Natural logarithm of biomass. d) Dissolved oxygen percentage, pH and agitation rate.

A correlation between *C. cohnii* dry cell weight (DCW in g/L), and the optical density at 470 nm (OD_{470}), was previously established, and can be found in Appendix B.

After the inoculation, the culture showed an exponential growth (Figure 3.1, a)), achieving a specific growth rate (μ_{max}) of 0.034 h^{-1} ($R^2 = 0.991$) (Figure 3.1, c)). The microalgae growth ceased at $t = 70.33 \text{ h}$, reaching at that time the maximum biomass concentration of 4.34 g/L , possibly as a result of oxygen limitation, as DO readings after $t = 48 \text{ h}$ were below 30% (Figure 3.1, d)). The highest biomass productivity ($P_{x \text{ max}}$) was achieved at $t = 52.62 \text{ h}$, with the value of 0.513 g/(L.h) (Figure 3.1, a), Table 3.1), while the average biomass productivity ($P_{x \text{ average}}$) was 0.059 g/(L.h) for the total batch time (73.75 h). Safdar *et al.* [37] also grew *C. cohnii* ATCC 30555 on pure glycerol in 1 L fermenter for lipid production and reported a biomass concentration of 15.1 g/L DCW , and a μ_{max} of 0.72 d^{-1} (0.03 h^{-1}), similar to this work. Hosoglu and Elibol [36] reported a final cell dry weight around $5.7\text{-}7.3 \text{ g/L DCW}$ and a $P_{x \text{ max}}$ of 1.0 g/L.d (0.042 g/(L.h)) for *C. cohnii* CCMP 316 cultivated in pure glycerol, in batch (2 L bioreactor,) higher than that obtained in this study, which may be explained by the higher glycerol purity used by those authors, since it should not contain inhibitor compounds. Other works reported *C. cohnii* biomass productivities between $0.72\text{-}1.0 \text{ g/(L.h)}$ when cultivated in different carbon sources, namely glucose, ethanol, carob pulp and acid acetic [87][31][27][88].

The speed rate (was maintained at low levels (250-300 rpm, Figure 3.1, d)), since this microalgae is particularly affected by the shear stress present in turbulent environments. Indeed, according to Yeung *et al.* [89], *C. cohnii* cell cycle may be disturbed by shear stress. The authors found that when the cells were grown at 150 rpm, a high proportion of cells were arrested in G1 phase, intermediate phase of the cell cycle between the end of cell division in mitosis and the start of DNA replication during S-phase; however, as the agitation ceased, the cells normally resumed the cell cycle.

The glycerol concentration decreased throughout the fermentation (Figure 3.1, b)), but was not depleted, reaching a final concentration of 11.97 g/L .

The DO decreased up to 30% at $t = 30 \text{ h}$. For $t > 30 \text{ h}$, the DO levels attained 20%, which might have led to oxygen limiting conditions in the broth, as above referred (Figure 3.1, d).

Table 3.1 - Kinetic parameters calculated for *C. cohnii* growth in Experiment I, according to the equations shown in the Materials and Methods Section

Kinetic parameter	Value	Unit
Specific growth rate, μ_{\max}	0.034	h^{-1}
Maximum biomass concentration	4.34	g/L
Maximum productivity in biomass $P_{X \max}$	0.513	g/(L.h)
Average productivity in biomass, $P_{X \text{ average}}$	0.059	g/(L.h)
Total lipid content (TFA)	24.61	% $W_{\text{TFA}}/W_{\text{biomass}}$
TFA yield, $Y_{\text{TFA}/S}$	0.00108	$W_{\text{TFA}}/W_{\text{glycerol}}$
Volumetric productivity in TFA, P_{TFA}	0.015	g/(L.h)
DHA content in biomass	8.20	% $W_{\text{DHA}}/W_{\text{biomass}}$
DHA Volumetric productivity	0.005	g/(L.h)
DHA content in TFA	33.36	% $W_{\text{DHA}}/W_{\text{TFA}}$
DHA yield $Y_{\text{DHA}/S}$	0.00036	$W_{\text{DHA}}/W_{\text{glycerol}}$
Biomass yield, $Y_{X/S}$	0.00424	$W_{\text{biomass}}/W_{\text{glycerol}}$
Substrate consumption volumetric rate, $-r_s$	0.18875	g/(L.h)

The total lipid content (measured as TFA) in this experiment was obtained only from the biomass collected at the end of the batch, attaining 24.61% ($W_{\text{TFA}}/W_{\text{biomass}}$), corresponding to a TFA concentration of 1.10 g/L, a TFA yield of 0.00108 $W_{\text{TFA}}/W_{\text{glycerol}}$ and a TFA productivity of 0.015 g/(L.h) (Table 3.1).

Table 3.2 shows *C. cohnii* fatty acid composition for experiment I. The DHA content in biomass was 8.20% ($W_{\text{DHA}}/W_{\text{biomass}}$) corresponding to a DHA concentration of 0.37 g/L, a productivity of 0.005 g/(L.h), DHA proportion in TFA of 33.36% ($W_{\text{DHA}}/W_{\text{TFA}}$) and DHA yield of 0.00036 $W_{\text{DHA}}/W_{\text{glycerol}}$. The results presented are in agreement with those described by Safdar *et al.* [37], who described *C. cohnii* ATCC 30555 cells cultured in a 1 L Fermenter under batch mode, over 7 days (168 h), reporting a TFA content of 26.4% ($W_{\text{TFA}}/W_{\text{biomass}}$) and a lipid productivity of 0.6 g/(L.d) (0.025 g/(L.h)), higher than that obtained for this work (0.015 g/Lh). The DHA proportion relatively to TFA was 39% ($W_{\text{DHA}}/W_{\text{TFA}}$). Hosoglu and Elibol [36] achieved TFA content of 30% ($W_{\text{TFA}}/W_{\text{biomass}}$) and an overall biomass yield of 0.30-0.48 ($W_{\text{biomass}}/W_{\text{glycerol}}$), significantly higher than those obtained in this work (0.00424 $W_{\text{biomass}}/W_{\text{glycerol}}$), which again might have been

due to oxygen limiting conditions that could occur during this cultivation, or the crude glycerol used in the present work.

The substrate uptake volumetric rate (r_s) obtained was 0.18875 g/(L.h); higher than that reported in the literature by Taborda *et al.* (0.1187 g/(L.h)) [33], which may be due to the different culture mode used, shake-flask cultures instead of the bioreactor.

DHA (22:6w3) was the dominant fatty acid in *C. cohnii* biomass collected at the end of the cultivation (33.36% w/w TFA) (Table 3.2). Other abundant FAs were the saturated fatty acids (SFAs) 12:0 (9.82% w/w TFA), 14:0 (20.29% w/w TFA), 16:0 (16.36% w/w TFA), and the monounsaturated fatty acid 18:1w9 (13.01% w/w TFA). The FAs 10:0, 18:0 and 18:2w6 and were present in smaller amounts (<1.98% w/w TFA). Safdar *et al.* [37] obtained a similar profile in fatty acids, especially the DHA proportion, which was also much higher than the remaining FA. SFAs have the highest percentage, 48.96% w/w TFA, followed by PUFAs with 35.34% w/w TFA and finally MUFAs, with 15.69% w/w TFA. For this alga, other authors have also reported similar results [25][26].

Table 3.2 - Fatty acid composition, as percentage of total fatty acids (%w/w TFA), obtained for assay I concerning *C. cohnii* ATCC 30772, grown in batch mode. Data represent the mean of two analyses (two independent samples, injected once).

Time (h)		73.75*
FAs (%w/w TFA)		
Capric	10:0	1.65±0.13
Lauric	12:0	9.82±0.73
Myristic	14:0	20.29±1.12
Palmitic	16:0	16.36±0.23
Stearic	18:0	0.84±0.15
Oleic	18:1w9	13.01±0.78
Linoleic	18:2w6	1.98±0.37
DHA	22:6w3	33.36±1.13
Others		2.68
Saturated fatty acids (SFA)		48.96
Polyunsaturated (≥2 double bonds) (PUFA)		35.34
Monounsaturated (1 double bond)(MUFA)		15.69

*End of the batch

Cell viability

Flow cytometry (FC) was used to investigate cell viability throughout cultivation. Figure 3.2 shows the results of the proportion of *C. cohnii* cells stained with PI and CFDA during Experiment I.

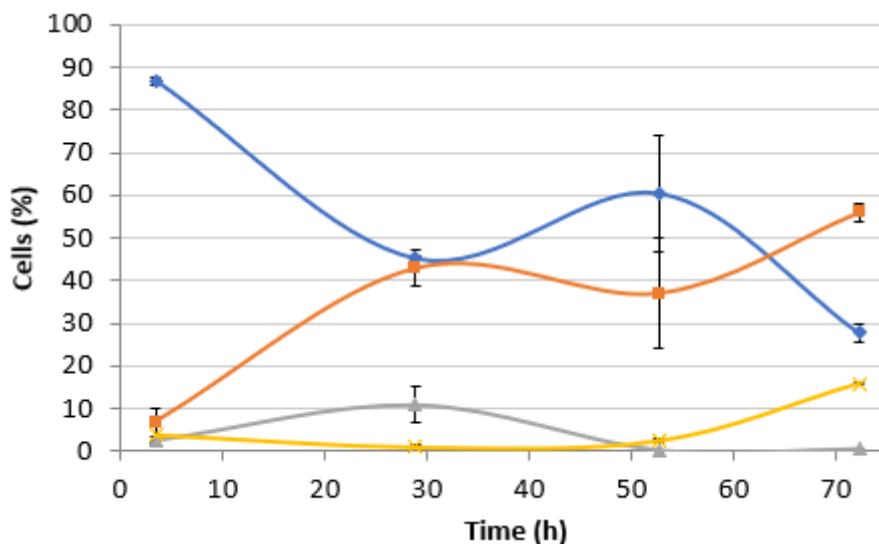


Figure 3.2 - Percentage of cells in each subpopulation, as defined in Introduction *Flow cytometry* chapter, for Experiment I. Cells were double stained with PI and CFDA. Subpopulation A (●) corresponds to cells with intact membrane and no enzymatic activity; Subpopulation B (■) comprises cells with intact membrane and enzymatic activity; Subpopulation C (▲) comprises cells with permeabilised membrane and enzymatic activity; Subpopulation D (×) comprises cells with permeabilised membrane and no enzymatic activity.

Figure 3.2 show that at the beginning of the experiment, the majority of cells (86.82%) had intact membrane and no enzymatic activity (subpopulation A) and decreased throughout the batch, reaching 27.72% at the end of the cultivation. This decrease was accompanied by an increase in subpopulation B (intact cells with enzymatic activity) that reached 55.96% at the end of the fermentation, revealing that the microalgae cells could adapt to the growth conditions. Indeed, at the end of the cultivation, the D and C stressed subpopulations were less than 15.86%, confirming that most of the cells were metabolically active.

3.1.2. Experiment II

In order to improve *C. cohnii* cell growth and lipid production, further fed-batch cultivations were carried out. The fed-batch mode has the advantage of extending the microalgae exponential growth phase, allowing to achieve higher cell densities, which cannot be obtained using batch cultures. For this reason, this technique is the most used in industry [47][34][28].

Figure 3.3 shows biomass concentration and biomass productivity, residual glycerol, the natural logarithm of the biomass, speed rate and DO, residual nitrogen, TFA/DHA content and DHA productivity profiles, over time, for Experiment II.

After the batch period, the feeding was performed whenever a decrease in biomass was detected, or no significant changes in growth were observed. The microalgae were cultured in batch mode from $t = 0$ h to $t = 102.75$ h (first green vertical traced line) and, from that time, a concentrated solution containing glycerol (carbon source) and other nutrients (composition in Materials and Methods Section) was added to the bioreactor.

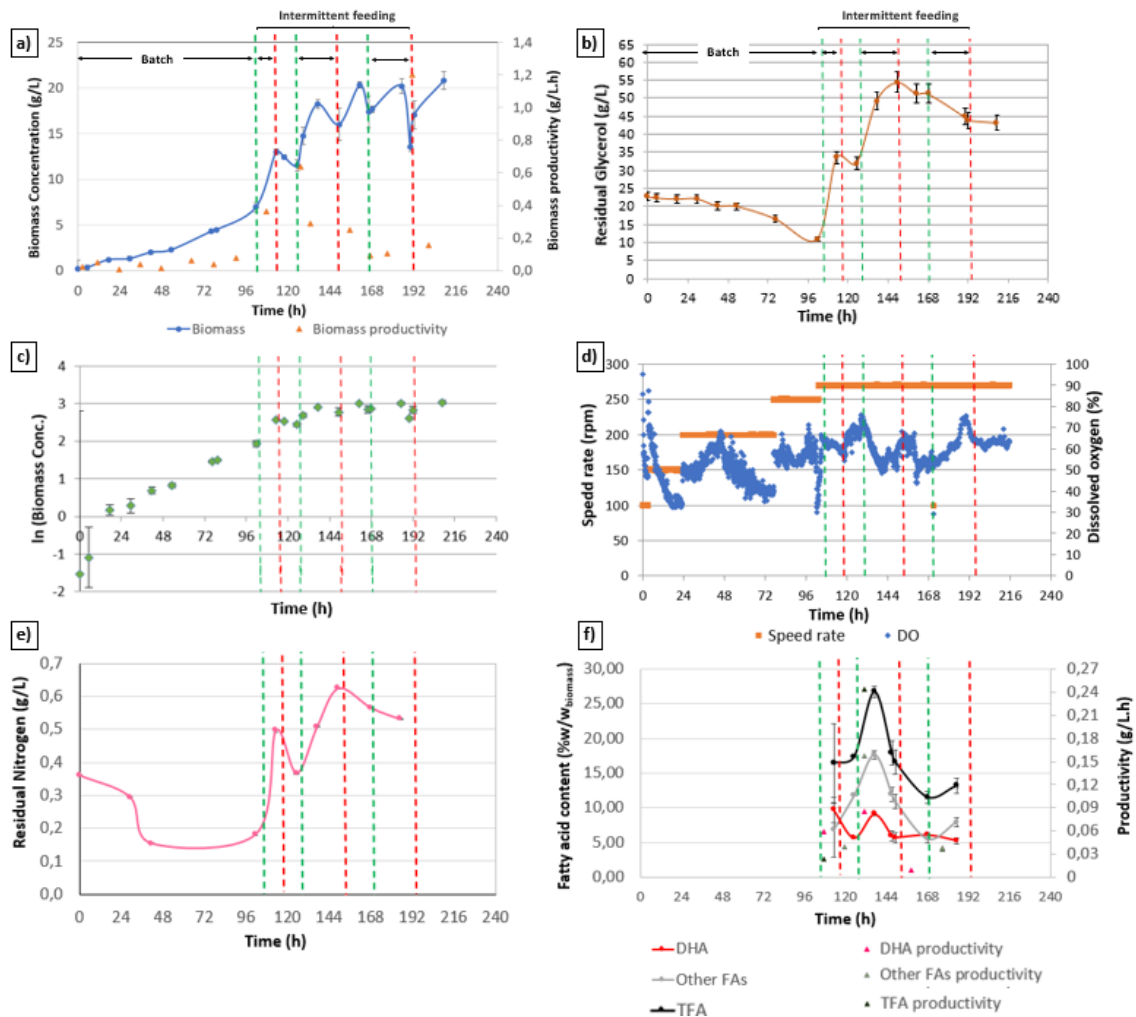


Figure 3.3 - *C. cohnii* ATCC 30772 growth in fed-batch mode (experiment II): a) Biomass concentration and productivity. b) Residual glycerol concentration. c) Natural logarithm of biomass. d) Dissolved oxygen percentage and agitation rate. e) Residual Nitrogen profile. f) TFA content, DHA and other lipids (%w/w_{biomass}), and respective productivities over time. The green vertical dashed line represents the feeding addition ($t = 102.75$ h, $t = 125.92$ h and $t = 166.42$ h) and the red dashed line represent interruptions of the substrate supply ($t = 113.00$ h, $t = 148.75$ h and $t = 200.0$ h). The black bars are deviations for each sample.

Unfortunately, due to technical limitations, the residual glycerol concentration was not available immediately after the sample collection, which did not allow the feeding rate adjustment, based on these results. Therefore, the feed rate adjustment was made whenever the microalgae growth ceased and the DO increased.

At the end of the batch culture, the biomass concentration attained 6.94 g/L (Figure 3.3, a)) and the residual glycerol concentration reached 10 g/L (Figure 3.3, b)). Thereafter the feeding was started, and the biomass concentration increased up to 20.82 g/L, at the end of the cultivation, corresponding to an average productivity of 0.07 g/L.h.

$P_{x \max}$ was 1.2 g/L.h at $t = 191.1$ h, when the biomass concentration attained 13.57 g/L. The μ_{\max} was calculated for the cultivation time $0 \text{ h} < t < 17.5 \text{ h}$ and $29.3 \text{ h} < t < 137 \text{ h}$, giving 0.059 h^{-1} and 0.024 h^{-1} , respectively. The specific growth rate decrease at $t = 24$ h could be due to the speed rate increase, as above referred (Yeung *et al.* [7]), since *C. cohnii* growth is affected by shear stress.

The crude glycerol and CSL contained a high proportion of particles that might have interfered in the biomass quantification, especially during the feeding stage, since a concentrated solution containing glycerol and CSL was feeding the bioreactor, which might have given overestimated biomass concentration results.

The residual glycerol concentration gradually increased with the feeding start, reached a maximum of 54.45 g/L at $t = 149.25$ h and decreased to 43.15 g/L at the end of the assay.

The residual nitrogen concentration reached minimum of 0.15 g/L $t = 41.67$ h and remained constant until the end of the batch phase. As the feeding started, it reached a maximum value of 0.63 g/L at $t = 149.25$ h and decreased again to 0.53 g/L at the end of the trial (Figure 3.3, e)).

The speed rate was adjusted according to the DO readings (between 200-270 rpm), which recorded values always above 30% (Figure 3.3, d)).

The TFA content varied between 11.54% w/w and 26.75% w/w during the assay (Figure 3.3, f)), with an average productivity of 0.00429 g/(L.h). As expected, after the batch phase ($t = 102.75$ h), *C. cohnii* started accumulating lipids, and the maximum TFA content (26.75% w/w DCW) was reached at $t = 137.08$ h, when the microalgae entered the stationary phase.

The highest DHA productivity (0.086 g/(L.h)) and DHA content (7.38% w/w DCW) was achieved at the same time ($t = 131.17$ h). These results were expected, as during the exponential growth phase, cells use carbon for cell division; as cells reach the stationary phase, they use the carbon in excess for lipidic storage materials, as a survival mechanism. Afterwards the DHA accumulation decreased, reaching 5.28% (w/w DCW) at $t = 185.08$ h, probably as a result of the high residual glycerol concentration in the broth, which might have inhibited the microalgal lipid synthesis.

The fed-batch fermentation strategy reported by De Swaaf *et al.* [34] in which *C. cohnii* ATCC 30772 was grown on glucose, resulted in final concentrations of 109 g/L dry biomass, 61 g/L lipids, and 19 g/L DHA using glucose as carbon source [34], further demonstrating that the capacity of microalgae to produce lipids. These results are higher than those obtained during the present work (6.96 g/L of maximum biomass concentration; 4.68 g/L of maximum lipid

concentration; and 1.26 g/L DHA concentration), which could be due to the raw glycerol used as carbon source in this work.

Table 3.3 - Kinetic parameters calculated for *C. cohnii* growth in Experiment II, according to the expressions shown in the Materials and Methods Section

Kinetic parameter	Value	Unit
Specific growth rate, μ_{max}	*0.059; 0.024	h^{-1}
Maximum biomass concentration (g/L)	20.82	g/L
Maximum productivity in biomass $P_{X_{max}}$	1.2	g/(L.h)
Average productivity in biomass, $P_{X_{average}}$	0.07	g/(L.h)
Total lipid content (TFA)	11.54 - 26.75	% $W_{TFA}/W_{biomass}$
Volumetric productivity in TFA, P_{TFA}	0.00429	g/(L.h)
DHA content in biomass	**7.38	% $W_{DHA}/W_{biomass}$
DHA Volumetric productivity	**0.086	g/(L.h)
DHA content in TFA	31.16-53.06	% W_{DHA}/W_{TFA}

*Cultivation time 0 h < t < 17.5 h and 29.3 h < t < 137 h, respectively.

** Maximum obtained at t = 131.17 h.

The fatty acid composition for *C. cohnii* saponifiable lipid fraction of was analysed to evaluate its potential as DHA and biodiesel sources. Table 3.4 shows the distribution of the FAs comprising the TFA content presented in Figure 3.3 f) as percentage of TFA, for experiment II performed in fed-batch.

The FAs proportions varied over the course of microalgae growth. In this assay, DHA proportion was always higher than 31.16%; myristic (14:0), palmitic (16:0), and oleic (18:1w9) acids also stood out displaying maximum percentages of 21.69% (w/w TFA at t = 113.25 h), 18.91% (w/w TFA at t = 147.25 h) and 20.77% (w/w TFA at t = 168.08 h), respectively. The percentages of myristic and palmitic fatty acids are in the range of the values published by De Swaaf [29] but oleic acid proportion was lower in that study (<10.1%).

The percentage of DHA steadily increased up to t = 149.25 h. Thereafter, it increased about 18% (w/w TFA), reaching a maximum of 53.06% (w/w TFA) at t = 168.08 h. At that moment, oleic, linoleic and stearic fatty acids also reached their maximum values (20.77%, 3.36%, 0.98% (w/w TFA), respectively). Myristic and palmitic acid reached their minimum values at this time, around 11.66% (w/w TFA) and 5.65% (w/w TFA), respectively. Capric acid decreased over the cultivation time course from 1.25% to 0.20% (w/w TFA). DHA accumulation pattern in *C. cohnii* ATCC 30772

observed during this assay was not entirely the same as that observed for the study reported by De Swaaf [29]. In that work, the DHA composition was always increasing until the end of the experiment, and the other fatty acids also evolved differently, such as linoleic acid which remained constant throughout the trial (approximately 10% (w/w TFA)).

In fact, it is known that the growth phase influences DHA production. Jiang and Chen [90] reported that, as the culture aged up to the early stationary phase, the DHA content increased. The changes in fatty acid composition, such as the DHA content increase, and the decrease in SFA content in the late exponential phase/ early stationary phase, might be the result of complete consumption or starvation of some specific nutrients by the cells, which induced FA composition changes. Sufficient nitrogen supply might lead to the synthesis of more SFA. On the contrary, nitrogen limitation might result in the formation of more unsaturated fatty acids [91]. In the present work, the nitrogen concentration was always lower than 0.7 g/L, which may explain the decrease in SFA and increase in PUFA, as the glycerol accumulated in the broth.

As already mentioned, this microalgae produces significant amounts of DHA, being the major PUFA in *C. cohnii* oil, which facilitate its extraction and purification.

Table 3.4 - Fatty acid composition, as percentage of total fatty acids (%w/w TFA), obtained for *C. cohnii* ATCC 30772, grown in fed-batch mode. Data represent the mean of two analyses (two independent samples, injected once over time (h)).

Time (h)		101.75	113.25	125.25	137.08	147.25	149.25	168.08	185.08
FAs (%w/w TFA)									
Capric	10:0	1.25±0.02	0.20±0.015	0.41±0.55	0.43±0.05	0.50±0.04	0.34±0.03	0.34±0.03	0.20±0.02
Lauric	12:0	9.42±0.12	8.66±0.00	7.84±0.03	5.25±0.06	4.85±0.02	4.60±0.05	4.11±0.55	2.72±0.11
Myristic	14:0	20.66±0.19	21.69±1.28	21.10±0.09	20.47±0.15	20.37±0.079	19.73±0.08	11.66±14.28	18.24±0.10
Palmitic	16:0	16.60±0.02	17.91±1.85	17.53±0.06	18.31±0.30	18.91±0.33	18.30±0.01	5.65±0.91	18.47±0.50
Stearic	18:0	0.72±0.01	0.85±0.24	0.71±0.01	0.81±0.06	0.80±0.01	0.75±0.03	0.98±0.15	0.78±0.03
Oleic	18:1w9	13.52±0.09	11.51±2.83	13.65±0.06	14.19±0.59	15.25±0.40	15.36±0.20	20.77±3.46	15.21±0.75
Linoleic	18:2w6	1.66±0.01	2.27±0.03	1.88±0.02	2.43±0.05	2.58±0.08	2.84±0.03	3.36±0.52	2.44±0.08
DHA	22:6w3	31.16±0.26	32.93±2.19	32.42±0.24	34.38±0.79	33.20±0.78	34.34±0.08	53.06±8.66	40.06±1.08
Others		5.01	3.97	4.46	3.73	3.54	3.75	0.06	1.88
Saturated fatty acids (SFA)		48.65	49.31	47.59	45.27	45.43	43.72	22.74	40.41
Polyunsaturated fatty acids (PUFA) (≥2 double bonds)		33.00	35.6	34.54	37.13	35.78	37.18	56.42	42.5
Monounsaturated fatty acids (MUFA) (1 double bond)		18.35	15.23	17.87	17.60	18.79	19.1	20.84	17.09

3.1.2.1. Estimations of Some Physical Parameters of *C. cohnii* SFA/MUFA Fraction

As mentioned before, biodiesel to be marketed in the European Union needs to comply within certain parameter values (Table A.1, Appendix C). Several parameters are only possible to estimate through experimental testing, but others can be estimated theoretically based only on the biodiesel composition obtained.

One of the goals of the OMEGAFUEL project is *C. cohnii* lipid fractionating, to obtain a DHA rich fraction, for pharmaceutical/food/cosmetic purposes, and another lipid fraction, rich in SFA/MUFA, for biodiesel purposes. There are several methods used to separate the PUFAs from MUFA/SFA. One methodology is described in EU patent EP2585570A1 (Kristinsson *et al.* [92]), which uses lipases promoting transesterification and short-path distillation to isolate the PUFAs from the residual FA fraction. Lopes da Silva *et al.* (2018) [93] described the co-extraction of ω -3 compounds and SFA/MUFA from fish canning by-products oil. To achieve this, winterization and urea complexation methods were used to obtain two fractions, one rich in saturated and monounsaturated fatty acids methyl esters (FAME) and the other in polyunsaturated FAME. The latter was then analysed by preparative HPLC analysis in order to concentrate ω -3 compounds. The remaining saturated fraction was considered as potential biodiesel. This methodology can be applied to microalgal oil.

In order to evaluate the potential of *C. cohnii* SFA+MUFA fraction, obtained at $t = 168.08$ h from assay II, for biodiesel purposes, according to the EU 14214 standard, several parameters, such as density, cetane number and viscosity (both dynamic and kinematic) were empirically estimated.

One of the parameters referred in the EU Standard is namely the saturation of PUFAs, which should not be higher than 3 double bonds and the Linolenic acid methyl ester should not be higher than 12.0% w/w. Table 3.5 shows *C. cohnii* SFA+MUFA fraction composition, weight fractions (w_i), the mole fractions (x_i) and the molecular weights (MW_i) [94]. According to this table, *C. cohnii* SFA/MUFA lipid fraction does not contain linolenic acid and does not contain FA with more than 3 double bonds.

Table 3.5 - *C. cohnii* SFA+MUFA fraction, FA composition, weight percentages (w_i), normalized molar fractions (x_i) and molecular weights (MW_i) [94].

		w_i (%)	x_i (%)	MW_i
FAs				
Capric	10:0	0.78	1.12	186.27
Lauric	12:0	9.45	11.74	214.32
Myristic	14:0	26.80	29.45	242.38
Palmitic	16:0	12.99	12.79	270.43
Stearic	18:0	2.25	2.01	298.48
Oleic	18:1ω9	47.74	42.89	296.47

Density

According to the EU standard 14214, the biodiesel density must vary between 860 and 900 kg/m³ at 15°C [63]. The density of the biodiesel fraction was estimated using the method described by Pratas *et al.* [83] in the Materials and Methods section.

Table 3.6 contains the A, B and C parameters for the four groups considered in a FAME (CH₂, CH₃, CH= and COO), as well as the calculated temperature-dependent molar volume Δv_i at 288 K (15 °C). This table also contains values of Δv_i at 313 K (40 °C), which will be used later in the calculation of the kinematic viscosity.

Table 3.6 - Parameters A, B and C [83], along with the temperature-dependent molar volume for each group considered in a FAME at 288 K (15 °C) and 313 K (40 °C).

	A	B	C	Δv_i at 288 K	Δv_i at 313 K
Groups					
CH ₂	12.04	0.0141	0	16.101	16.453
CH ₃	15.43	0.0556	0	31.451	32.833
CH=	11.43	0.0068	0	13.376	13.558
COO	61.15	-0.2482	0.000368	20.200	19.516

Table 3.7 contains number of groups for each group for each FAME considered in the group contribution method (GCVOL) [95].

Table 3.7. Number of groups for each of the considered groups corresponding to each fatty acid in the biodiesel fraction.

		Number of Groups			
FAs		CH ₂	CH ₃	CH=	COO
Capric	10:0	8	2	0	1
Lauric	12:0	10	2	0	1
Myristic	14:0	12	2	0	1
Palmitic	16:0	14	2	0	1
Stearic	18:0	16	2	0	1
Oleic	18:1 ω 9	14	2	2	1

Solving Equation (12) and (13) for each FAME and with their molar weights gives a molar volume of 302.51 cm³/mol and a density of 880.54 kg/m³. This value is within the requirements given by the EU.

Kinematic Viscosity

In the EU Standard 14214 the kinematic viscosity of a given biodiesel should be between 3.5 and 5.0 mm²/s at 40 °C (313 K). The density of the SFA+MUFA fraction was estimated using the method described by Freitas *et al.* in the Materials and Methods section, but with the temperature at 40°C instead of 15°C, to calculate this parameter for the same temperature as the reference value. A result of 861.22 kg/m³ was obtained.

The parameters for the Yuan model revised by Freitas *et al.* (2011) for the FAME present in the biodiesel fraction are shown in Table 3.8.

Table 3.8. Parameters A, B and T₀ considered for each of the FAMES present in the biodiesel fraction.

FAs		A	B	T ₀
Capric	10:0	-3.316	814.674	93.317
Lauric	12:0	-3.089	767.388	112.267
Myristic	14:0	-3.124	837.282	112.358
Palmitic	16:0	-2.808	746.528	132.676
Stearic	18:0	-2.985	876.221	122.303
Oleic	18:1 ω 9	-2.7	748.184	129.249

Solving (16) for all FAMES and using these results in Equation (15) gives a dynamic viscosity of 3.54 mPa.s. Dividing this value by the previously estimated density (for T = 313 K) gives a kinematic viscosity of 4.11 mm²/s (equation (14)), which is within EU regulations [63].

Cetane Number

According to EU Standard 14214, the cetane number of a biodiesel should be higher than 51 [63].

From Equation (18) and (19) gives a DU of 47.74 and a SCSF of 1.28. Using these values to solve (17) results in a cetane number of 59.77, which is above the lower limit of the EU standard referred to in Appendix C.

Cell viability

Figure 3.4 shows cell viability during Experiment II, using the double staining method with CFDA and PI.

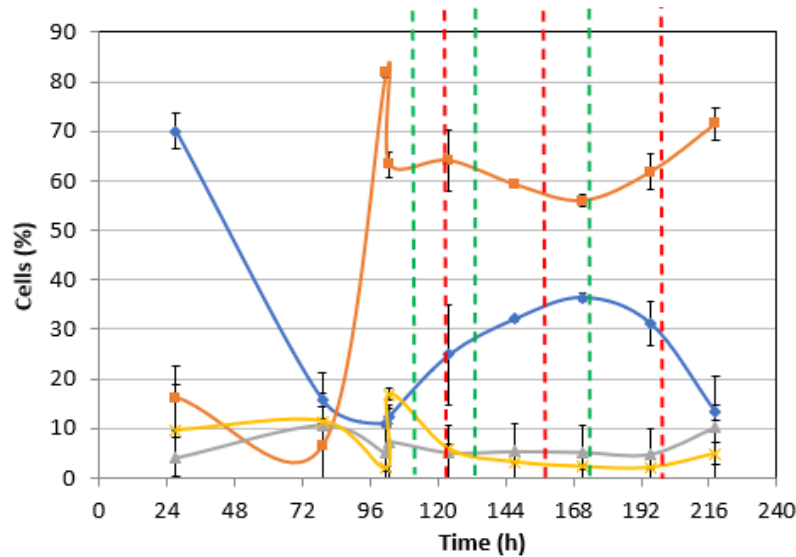


Figure 3.4 - Percentage of cells in each subpopulation for Experiment II, as defined in Figure 3.2. Cells were stained with PI and CFDA. The green vertical dashed line represents the feeding start ($t = 102.75$ h, $t = 125.92$ h and $t = 166.42$ h), the red vertical dashed line indicates that the feeding was suspended ($t = 113.00$ h, $t = 148.75$ h and $t = 200.0$ h). Subpopulation A (●) corresponds to cells with intact membrane and no enzymatic activity; Subpopulation B (■) comprises cell with intact membrane and enzymatic activity; Subpopulation C (▲) comprises cells with permeabilised membrane and enzymatic activity; Subpopulation D (×) cells with permeabilised membrane and no enzymatic activity.

Subpopulation A, consisting of cells with intact membrane and no enzymatic activity, was dominant at the beginning of the experiment (70%), decreasing throughout the experiment before the feeding started. However, at the end of the batch mode, ($t = 102.75$ h), most cells (63.33%) had intact cytoplasmic membrane and enzyme activity (subpopulation B), indicating that most cells were not exposed to adverse conditions until the end of the culture, where this subpopulation reached 71.58%. Subpopulations C and D, both with permeabilised cytoplasmic membranes, remained at low percentages, less than 20%, demonstrating that the crude glycerol, used as carbon source in the medium formulation for *C. cohnii* growth, did not significantly affect the microalgae metabolism.

3.1.3. Experiment III

The crude glycerol and the CLS contained a high proportion of particles, which might have interfered with the biomass quantification. One possibility to get rid of undesirable particles from the media containing particles consists of centrifuging the media before inoculation. However, this step is time-consuming and expensive, and infeasible for large media volumes.

During this experiment, the biomass concentration quantification was performed by two methods: dry cell weight and (Figure 3.5, a)) and by cell counting, using flow cytometry (Figure 3.5, b)), since this technique allows discriminating the microalgae cells population from the background.

A correlation between the cell number (cells/mL) obtained by FC, and the optical density (OD₄₇₀) was previously established. Additionally, a correlation was established between cell number and cell dry weight (g/L) (Appendix B), and the one used so far, between DCW and OD₄₇₀.

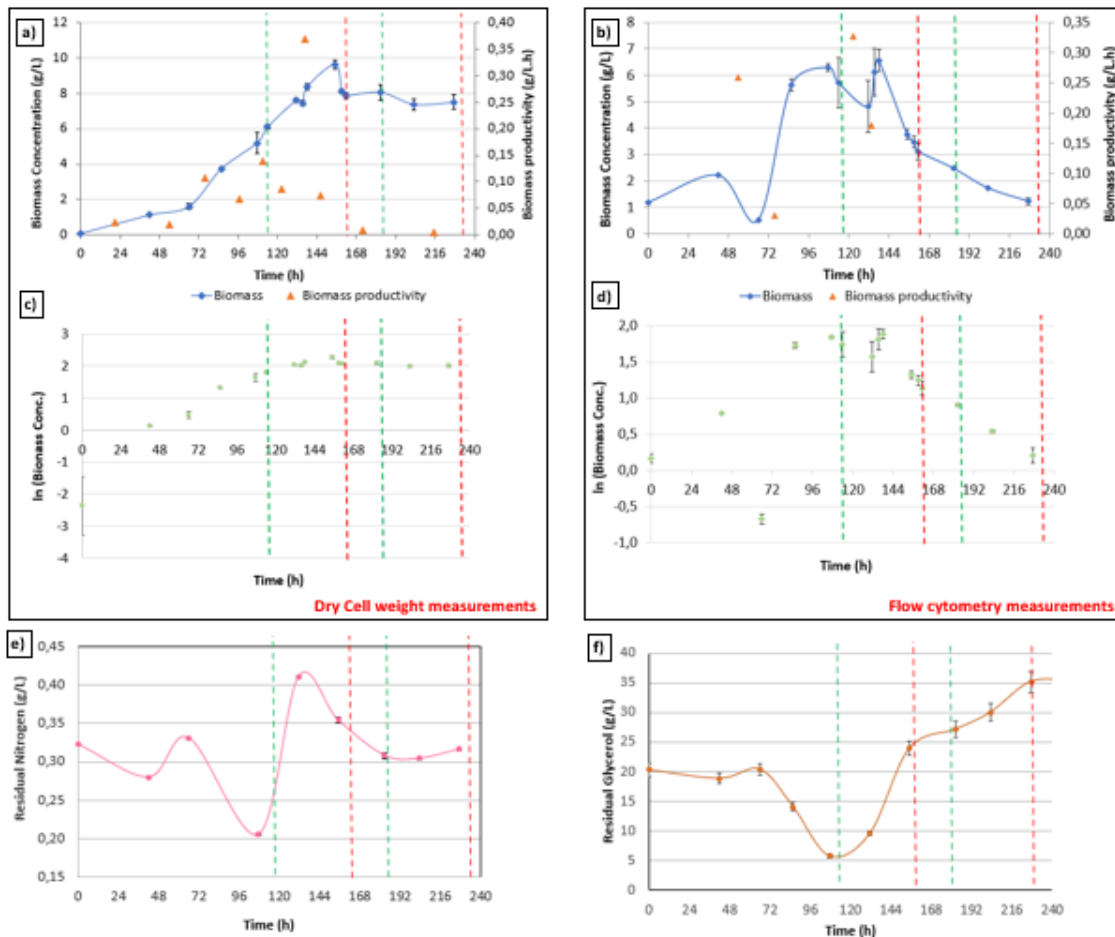


Figure 3.5 - *C. cohnii* ATCC 30772 growth in fed-batch mode (experiment III): a) Biomass concentration determined by optical density and productivity b) Biomass concentration determined by Flow cytometry and biomass productivity c) Profile of the natural logarithm of biomass determined by optical density d) Profile of the natural logarithm of biomass determined by Flow cytometry e) Residual Nitrogen profile (g/L) and f) Residual glycerol profile (g/L), over time. The green vertical dashed line represents the feeding start (t = 114.50 h and t = 185.45 h) and the red dashed line represent interruptions of the substrate supply (t = 162.50 h and t = 233.30 h). The black bars are standard deviation for each sample.

Comparing the biomass concentration values obtained by the two methods, they are quite disparate, although the flow cytometry results should be, in principle, more reliable.

The biomass concentration results obtained by the two methods reached a maximum, after the feeding start, of 9.63 g/L and 6.56 g/L, for DCW and FC, respectively, when the residual nitrogen and carbon were in excess in the broth. As expected, the biomass concentration values were higher when determined by dry cell weight, comparing to those obtained by FC. In addition, the biomass

concentration determined by FC decreased pronouncedly, after $t = 144$ h, while maintained a plateau, when determined by DCW.

The batch phase was extended compared to the other two trials, up to $t = 114.0$ h, corresponding to a biomass concentration of 6.10 g/L (measured by DCW, Figure 3.5, a)), with a maximum biomass productivity of 0.37 g/(L.h) for $t = 136.75$ h and the maximum biomass concentration was reached at $t = 155.0$ h of 9.63 h/L. The specific growth rate was 0.059 h⁻¹ (calculated for the period of 0 h < t < 42 h) and 0.026 h⁻¹ (calculated for the time period of 66.0 h < t < 114.0 h).

Table 3.9 - Kinetic parameters calculated for *C. cohnii* growth in Experiment III, according to the expressions shown in the Materials and Methods Section.

Kinetic parameter	Value		Unit
	DCW	FC	
Specific growth rate, m_{\max}	*0.059; 0.026	*0.015; 0.047	h ⁻¹
Maximum biomass concentration (g/L)	9.63	6.56	g/L
Maximum productivity in biomass $P_{X \max}$	0.37	0.33	g/(L.h)
Average productivity in biomass, $P_{X \text{ average}}$	0.0325	0.00023	g/(L.h)

* 0 h < t < 42 h and 66.0 h < t < 114.0 h, respectively.

On the other hand, according to the FC results, the specific growth rate was 0.015 h⁻¹ (0 h < t < 42 h) and 0.047 h⁻¹ (66.0 h < t < 114.0 h), and the maximum biomass productivity was 0.33 g/(L.h) at $t = 122.75$ h.

Unfortunately, there were some problems with the monitoring software, and the stirring rate, DO and pH could not be recorded. However, the pH was maintained at the same value as previous experiment (6.5) and stirring rate was also adjusted, between 100-300 rpm. To prevent substrate (carbon) inhibition, the feeding flow rate was 0.02 L/h, lower than in experiment II (0.03 L/h). In fact, the residual glycerol level, as the batch phase was longer, reached minimum values close to 5 g/L. However, during the feeding stage, the residual glycerol concentration gradually rose until the end of the experiment, attaining 35.24 g/L at $t = 251.3$ h, which could explain the microalgae growth stop.

The percentage of nitrogen (Figure 3.5, e)) decreased along the batch phase, reaching minimum values of 0.21 g/L at $t = 107.50$ h. After the feeding start, it increased reaching maximum values at $t = 131.50$ h of 0.41 g/L, then stabilised and remained approximately constant until the end of the experiment (0.30 - 0.33 g/L).

If the media contain particles, the biomass concentration quantification may be affected by them, giving overestimated results. Flow cytometry should be more reliable than DCW measurements for

monitoring culture growth since it only takes into account *C. cohnii* cells (contrarily to DCW measurements which does not distinguish cells from other particles).

Cell viability

As observed for the previous experiments, initially most of *C. cohnii* cells had intact membrane and no enzymatic activity (subpopulation A), 64.86% at $t = 67$ h. Over the course of the assay, these cells decreased reaching a minimum at of 22.14%, at $t = 155.0$ h, giving way to subpopulations of B (composed of healthy cells) and D (composed of cells with permeabilised membrane and no enzymatic activity). Subpopulation D substantially increased from 15.35% at $t = 67$ h until 73.21% at $t = 155$ h, indicating that, at that time, cells underwent stress conditions. In fact, the increase in subpopulation C was coincident with the decrease in subpopulation A (which attained 22.14% at $t = 155$ h) and the decrease in subpopulation B (which attained 3.73% at $t = 155$ h). At the same time, the residual glycerol concentration increased, attaining 35.16 g/L at $t = 227.3$ h) which was accompanied by a decrease in biomass concentration until the end of the cultivation (1.23 g/L at $t = 227.3$ h). These results suggested that *C. cohnii* membrane integrity and enzymatic system were seriously affected during the period $72 \text{ h} < t < 144 \text{ h}$, leading to the microalgal growth stop, probably due to oxygen limitation (unfortunately no DO readings could be obtained during this assay). From $t = 155$ h until the end of the cultivation, the proportion of cells with permeabilised membrane (subpopulation D) varied from 73.21% until 27.16%.

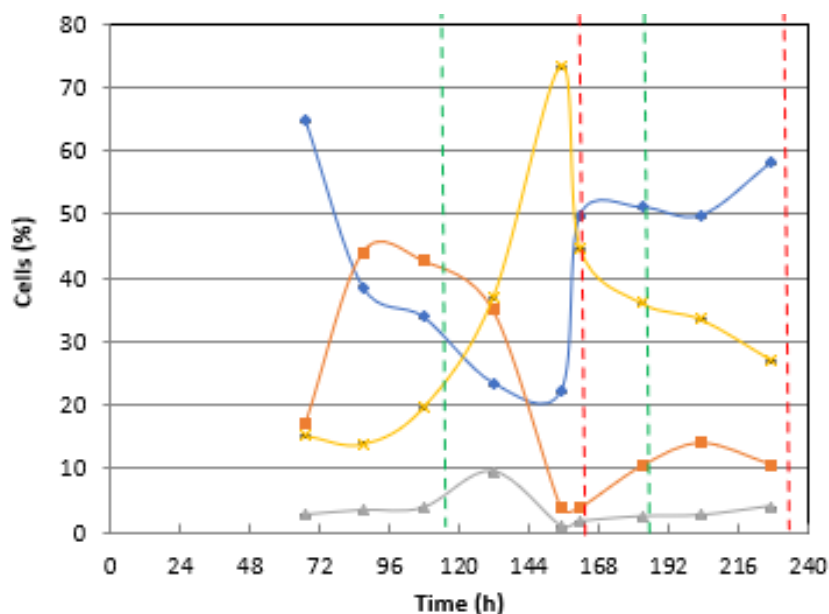


Figure 3.6 - Percentage of cells in each subpopulation for Experiment III. Cells were stained with PI and CFDA. The green vertical dashed line represents the start of culture feeding ($t = 114.50$ h and $t = 185.05$ h) and whenever there is a red vertical dashed line the feeding was suspended ($t = 162.50$ h and $t = 233.30$ h). Subpopulation A (●) correspond to cells with intact membrane and no enzymatic activity; Subpopulation B (■) comprise cell with intact membrane and enzymatic activity; Subpopulation C (▲) are cells with permeabilised membrane and enzymatic activity; Subpopulation D (×) cells with permeabilised membrane and no enzymatic activity.

Subpopulation A increased up to 60% at the end of the cultivation, suggesting that *C. cohnii* cells could recover from the stresses status (at least in terms of membrane integrity) resulted from adverse conditions that experienced during the first 168 h of cultivation. Despite the data loss that occurred during this experiment, it allowed to conclude that the use of FC for *C. cohnii* biomass concentration determination is possible and should be more reliable than DCW measurements.

4. Conclusions and Next Steps

The main objective of this work was to determine an experimental protocol to optimise the cultivation of *Cryptocodinium cohnii* ATCC 30772 in fed-batch cultures, in a benchtop bioreactor, to achieve high cell density and lipids, as a source of docosahexaenoic acid (DHA) and biodiesel. Furthermore, it also aimed, on one hand, to study the ability to monitor microalgae cultivation parameters, such as biomass growth and cell viability by optical density and flow cytometry, to establish a correlation between biomass, optical density and cell number and, on the other hand, also to demonstrate the potential of crude glycerol as a carbon source to grow this heterotrophic microalgae.

Three assays were performed: one in batch and two in fed-batch mode. Regarding one of the mentioned objectives, *C. cohnii* grew on crude glycerol demonstrating that this substrate can be used as an alternative to commercial glucose, carbon source that is widely used in media formulations for microbial growth, including this microalgae, as described in the literature. This approach will result in the production costs decrease, as well as environmental benefits, since an industrial by-product is reused, according to the circular economy rules. Taborda [77] carried out an economic feasibility analysis and proved this using models that included several low-cost carbon sources, in which glycerol was a promising source, with gross profit margins of around 95.1%, a scenario in which glycerol, the by-product of biodiesel industry, is obtained in a circular economy context, with zero waste.

Flow cytometry was useful in monitoring cell growth as well as the physiological state of the algae throughout the assays; moreover, it revealed that the cells did not show high levels of stress, which confirms that crude glycerol did not drastically affect their metabolic activity, at least in terms of enzyme activity and cell membrane integrity. In experiment II, compared to experiment I, the biomass concentration increased 5-fold, reaching 20.82 g/L, an expected increase given that the objective of the fed-batch implementation was exactly to prolong the growth phase. However, considering that a concentrated nutrient solution containing crude glycerol and CLS was added to the broth, it is thought that part of this biomass could be due to particles present in the medium, although the OD and dry weight of the medium without cells were subtracted from the OD of the samples taken throughout the experiment.

Indeed, the particles interference in the biomass concentration quantification was particularly severe during the fed-batch fermentations, since under these conditions it is more difficult to subtract the OD/DCW values from the medium without cells, since the addition of the medium was continuous. Thus, during assay III attempts were made to overcome this problem, by cell counting using FC, which was considered to give more reliable results. One strategy to overcome the particles in the medium could be, for instance, to filter or centrifuge the feed medium first to remove the suspended particles; however, this step would add further complexity and increase the associated costs, particularly at a larger scale.

Unfortunately, due to the lockdown following the Covid-19 pandemic that started at 11.01.2021, it was not possible to optimise the growth conditions for this microalgae. Hence, the conclusions from

trial III were sparse and it was not possible to repeat this assay. Moreover, other problems were also encountered in this trial, namely in the process monitoring software, which malfunctioned: Also, it was not possible to quantify the lipids.

During the exponential phase, cells use carbon for cell division. When entering the stationary phase, they use the excess carbon for lipid production, which was verified in experiment II. Nevertheless, in experiment I, a DHA content of 8.20% ($W_{DHA}/W_{biomass}$) in biomass was obtained, higher than the maximum value obtained in experiment II, 7.38% ($W_{DHA}/W_{biomass}$), most probably due to substrate inhibition as a result of the uncontrolled nutrient addition after the batch phase.

Regarding the physical parameters determined for a biodiesel fraction from experiment II, all are within the limits stipulated by the EU Standard, which envisages the possibility of using this microalgae as a source of biodiesel, beyond the well-known source of the DHA.

The next steps of this work are related to *C. cohnii* lipid fractionating, in order to obtain a rich DHA lipidic fraction for pharmaceutical purposes, and a saturated/monounsaturated lipid fraction that may be potential used for biodiesel. However, before this step, it is necessary to refine the working methodology, namely cellular concentration monitorization by flow cytometry. An alternative way to monitor cell counting may include the use of specific dyes, such as Thiazole Orange, that allows estimating, by fluorescence intensity, the total amount of nucleic acids, making the distinction between the particles in the medium and the cells.

In terms of fed-batch optimisation, other equally cheap sources should be explored, such as sugarcane molasses. A real-time method for residual substrate quantification in the medium would be useful to avoid growth substrate inhibition.

5. References

- [1] S. Fernando, S. Adhikari, C. Chandrapal, and N. Murali, 'Biorefineries : Current Status, Challenges, and Future Direction', *Energy & Fuels*, no. 3, pp. 1727–1737, 2006.
- [2] F. Cherubini, 'The biorefinery concept: Using biomass instead of oil for producing energy and chemicals', *Energy Convers. Manag.*, vol. 51, no. 7, pp. 1412–1421, 2010.
- [3] M. Hingsamer and G. Jungmeier, 'Biorefineries', *Role Bioenergy Emerg. Bioeconomy*, pp. 179–222, 2019.
- [4] B. Kamm and M. Kamm, 'Biorefinery - systems', *Chem. Biochem. Eng. Q.*, vol. 18, no. 1, pp. 1–6, 2004.
- [5] R. Van Ree and B. Annevelink, 'Status Report Biorefinery 2007', *Agrotechnology Food Sci. Gr.*, 2007.
- [6] E. de Jong and G. Jungmeier, 'Biorefinery Concepts in Comparison to Petrochemical Refineries', *Ind. Biorefineries White Biotechnol.*, pp. 3–33, 2015.
- [7] R. Möller and D. Clayton, 'Micro- and macro-algae: utility for industrial applications', *CPL Press*, no. September, pp. 1–68, 2007.
- [8] K. A. Jung, S. Lim, Y. Kim, and J. Moon, 'Bioresource Technology Potentials of macroalgae as feedstocks for biorefinery', *Bioresour. Technol.*, vol. 135, pp. 182–190, 2013.
- [9] C. Filote, S. C. R. Santos, V. I. Popa, C. M. S. Botelho, and I. Volf, 'Biorefinery of marine macroalgae into high- tech bioproducts: a review', *Environ. Chem. Lett.*, vol. 19, pp. 969–1000, 2020.
- [10] T. Lopes, L. Gouveia, and A. Reis, 'Integrated microbial processes for biofuels and high value-added products : the way to improve the cost effectiveness of biofuel production', *Appl. Microbiol. Biotechnol.*, vol. 98, 2013.
- [11] E. J. Olguín, 'Dual purpose microalgae–bacteria-based systems that treat wastewater and produce biodiesel and chemical products within a Biorefinery', *Biotechnol. Adv.*, 2012.
- [12] J. K. Pittman, A. P. Dean, and O. Osundeko, 'Bioresource Technology The potential of sustainable algal biofuel production using wastewater resources', *Bioresour. Technol.*, vol. 102, no. 1, pp. 17–25, 2011.
- [13] P. R. F. Marcelino *et al.*, 'Industrial Crops & Products Biosurfactants production by yeasts using sugarcane bagasse hemicellulosic hydrolysate as new sustainable alternative for lignocellulosic biorefineries', *Ind. Crop. Prod.*, vol. 129, pp. 212–223, 2019.
- [14] R. P. John, G. S. Anisha, K. M. Nampoothiri, and A. Pandey, 'Bioresource Technology Micro and macroalgal biomass: A renewable source for bioethanol', *Bioresour. Technol.*, vol. 102, no. 1, pp.

- 186–193, 2011.
- [15] D. Fozer, N. Valentinyi, L. Racz, and P. Mizsey, 'Evaluation of microalgae-based biorefinery alternatives', *Clean Technol. Environ. Policy*, vol. 19, pp. 501–515, 2016.
- [16] L. Reijnders, 'Lipid-based liquid biofuels from autotrophic microalgae: energetic and environmental performance', *Wires Energy Environ.*, vol. 2, no. 1, pp. 73–85, 2012.
- [17] J. R. Benemann, I. Woertz, and T. Lundquist, 'Autotrophic Microalgae Biomass Production: From Niche Markets to Commodities', *Ind. Biotechnol.*, vol. 14, no. 1, pp. 3–10, 2018.
- [18] T. Lopes and C. Silva, 'The Role of Heterotrophic Microalgae in Waste Conversion to', *Processes*, vol. 9, pp. 1–24, 2021.
- [19] C. A. BEAM and M. HIMES, 'Distribution of Members of the *Cryptocodinium cohnii* (Dinophyceae) Species Complex', *J. Protozool.*, vol. 29, no. 1, pp. 8–15, 1982.
- [20] M. Ucko, M. Ucko, M. Elbrächter, and E. Schnepf, 'A *cryptocodinium cohnii*-like dinoflagellate feeding myzocytotically on the unicellular red alga porphyridium sp.', *Eur. J. Phycol.*, vol. 32, no. 2, pp. 133–140, 1997.
- [21] T. Lopes and C. Silva, 'The Dark Side of Microalgae Biotechnology : A Heterotrophic Biorefinery Platform Directed to ω -3 Rich Lipid Production', *Microorganisms*, vol. 7, pp. 1–21, 2019.
- [22] A. Mendes, A. Reis, and R. Vasconcelos, '*Cryptocodinium cohnii* with emphasis on DHA production : a review', *J. Appl. Phycol.*, vol. 21, 2008.
- [23] D. Pleissner and N. T. Eriksen, 'Effects of phosphorous, nitrogen, and carbon limitation on biomass composition in batch and continuous flow cultures of the heterotrophic dinoflagellate *Cryptocodinium cohnii*', *Biotechnol. Bioeng.*, vol. 109, no. 8, pp. 2005–2016, 2012.
- [24] C. Ratledge, 'Fatty acid biosynthesis in microorganisms being used for Single Cell Oil production', *Biochimie*, vol. 86, no. 11, pp. 807–815, 2004.
- [25] D. Marine, 'Lipid Composition and Biosynthesis in the marine dinoflagellate *Cryptocodinium cohnii*', vol. 27, no. 6, pp. 0–4, 1988.
- [26] Y. Jiang, F. Chen, and S. Liang, 'Production potential of docosahexaenoic acid by the heterotrophic marine dinoflagellate *Cryptocodinium cohnii*', vol. 34, pp. 633–637, 1999.
- [27] C. Ratledge, K. Kanagachandran, A. J. Anderson, D. J. Grantham, and J. C. Stephenson, 'Production of Docosahexaenoic Acid by *Cryptocodinium cohnii* Grown in a pH-Auxostat Culture with Acetic Acid as Principal Carbon Source', vol. 36, no. 11, pp. 7–12, 2001.
- [28] M. E. D. S. J. T. P. L. Sijtsma, 'Fed-batch cultivation of the docosahexaenoic-acid-producing marine alga *Cryptocodinium cohnii* on ethanol', pp. 40–43, 2003.
- [29] M. E. De Swaaf, 'Docosahexaenoic acid production by the marine alga *Cryptocodinium cohnii*',

Delft Univ. Press, no. May 2014, pp. 1–136, 2003.

- [30] Y. Gong *et al.*, 'Improvement of Omega-3 Docosahexaenoic Acid Production by Marine Dinoflagellate *Cryptocodinium cohnii* Using Rapeseed Meal Hydrolysate and Waste Molasses as Feedstock', *PLoS One*, vol. 10, pp. 1–18, 2015.
- [31] A. Mendes, A. P. Guerra, F. Ruano, and A. T. Lopes, 'Study of docosahexaenoic acid production by the heterotrophic microalga *Cryptocodinium cohnii* CCMP 316 using carob pulp as a promising carbon source', *World J Microbiol Biotechnol*, vol. 23, pp. 1209–1215, 2007.
- [32] M. Isleten-hosoglu, 'Bioutilization of Cheese Whey and Corn Steep Liquor by Heterotrophic Microalgae *Cryptocodinium cohnii* for Biomass and Lipid Production', *Acad. Food J.*, vol. 15, no. 3, pp. 233–241, 2017.
- [33] T. Taborda, P. Moniz, A. Reis, and T. L. da Silva, 'Evaluating low-cost substrates for *Cryptocodinium cohnii* lipids and DHA production, by flow cytometry', *J. Appl. Phycol.*, vol. 33, no. 1, pp. 263–274, 2021.
- [34] M. E. De Swaaf, L. Sijtsma, and J. T. Pronk, 'High-cell-density fed-batch cultivation of the docosahexaenoic acid producing marine alga *Cryptocodinium cohnii*', *Biotechnol. Bioeng.*, vol. 81, no. 6, pp. 666–672, 2003.
- [35] W. Safdar *et al.*, 'Growth kinetics , fatty acid composition and metabolic activity changes of *Cryptocodinium cohnii* under different nitrogen source and concentration', *AMB Express*, vol. 7, no. 1, pp. 1–15, 2017.
- [36] R. B. Letters, T. Campus, and T. Campus, 'Improvement of medium composition and cultivation conditions for growth and lipid production by *Cryptocodinium cohnii*', *Rom. Biotechnol. Lett.*, vol. 22, no. 6, 2017.
- [37] W. Safdar, X. Zan, and Y. Song, 'Synergistic Effects effects of pH , Temperature and Agitation on Growth Kinetics and Docosahexaenoic Acid Production of *C. cohnii* Cultured on Different Carbon Sources', *Int. J. Res. Agric. Sci.*, vol. 4, pp. 94–101, 2017.
- [38] M. 21228 (US) Kyle, David John Catonsville, 'EUROPEAN PATENT SPECIFICATION EP 1 419 780 B1', 04075413.7, 2009.
- [39] S. J. Sarma, G. S. Dhillon, S. K. Brar, Y. Le Bihan, G. Buelna, and M. Verma, 'Investigation of the effect of different crude glycerol components on hydrogen production by *Enterobacter aerogenes* NRRL B-407', *Renew. Energy*, vol. 60, pp. 566–571, 2013.
- [40] L. Sijtsma, A. J. Anderson, and C. Ratledge, 'Alternative Carbon Sources for Heterotrophic Production of Docosahexaenoic Acid by the Marine Alga *Cryptocodinium cohnii*', *Single Cell Oils*, pp. 131–149, 2010.
- [41] S. Chozhavendhan, G. K. Devi, B. Bharathiraja, R. P. Kumar, and S. Elavazhagan, 'Assessment of crude glycerol utilization for sustainable development of biorefineries', *Refin. Biomass*

Residues Sustain. Energy Bioprod., pp. 195–212, 2020.

- [42] S. Abad and X. Turon, 'Valorization of biodiesel derived glycerol as a carbon source to obtain added-value metabolites: Focus on polyunsaturated fatty acids', *Biotechnol. Adv.*, vol. 30, no. 3, pp. 733–741, 2012.
- [43] A. H. Metherel, A. F. Domenichiello, A. P. Kitson, K. E. Hopperton, and R. P. Bazinet, 'Biochimica et Biophysica Acta Whole-body DHA synthesis-secretion kinetics from plasma eicosapentaenoic acid and alpha-linolenic acid in the free-living rat', *BBA - Mol. Cell Biol. Lipids*, vol. 1861, no. 9, pp. 997–1004, 2016.
- [44] L. Lauritzen, P. Brambilla, A. Mazzocchi, L. B. S. Harsløf, V. Ciappolino, and C. Agostoni, 'DHA Effects in Brain Development and Function', *Nutrients*, vol. 8, no. 1, pp. 1–17, 2016.
- [45] M. Sprague, G. Xu, M. B. Betancor, R. E. Olsen, B. D. Glencross, and D. R. Tocher, 'Endogenous production of n-3 long-chain PUFA from first feeding and the influence of dietary linoleic acid and the α -linolenic:linoleic ratio in Atlantic salmon (*Salmo salar*)', *Br. J. Nutr.*, vol. 122, pp. 1091–1102, 2019.
- [46] S. D. Doughman, S. Krupanidhi, and C. B. Sanjeevi, 'Omega-3 Fatty Acids for Nutrition and Medicine : Considering Microalgae Oil as a Vegetarian Source of EPA and DHA', *Curr. Diabetes Rev.*, vol. 3, pp. 198–203, 2007.
- [47] F. Industries, 'Microalgae n-3 PUFAs Production and Use in Food and Feed Industries', *Mar. Drugs*, vol. 19, pp. 1–29, 2021.
- [48] A. F. Domenichiello, A. P. Kitson, and R. P. Bazinet, 'Is docosahexaenoic acid synthesis from a -linolenic acid sufficient to supply the adult brain?', *Prog. Lipid Res.*, vol. 59, pp. 54–66, 2015.
- [49] Y. Ma *et al.*, 'The Effect of Omega-3 Polyunsaturated Fatty Acid Supplementations on anti-Tumor Drugs in Triple Negative Breast Cancer The Effect of Omega-3 Polyunsaturated Fatty Acid Supplementations on anti-Tumor Drugs in Triple Negative Breast Cancer', *Nutr. Cancer*, vol. 0, no. 0, pp. 1–10, 2020.
- [50] A. Hassan, 'Prescription omega-3 fatty acid products : considerations for patients with diabetes mellitus', *Diabetes, Metab. Syndr. Obes. targets Ther.*, vol. 9, pp. 109–118, 2016.
- [51] F. Camacho and A. Macedo, 'Potential Industrial Applications and Commercialization of Microalgae in the Functional Food and Feed Industries : A Short Review', *Mar. Drugs*, vol. 17, pp. 17–312, 2019.
- [52] M. P. J. van der Voort, J. Spruijt, J. Potters, P. L. de Wolf, and H. J. H. Elissen, 'Socio-economic assessment of Algae-based PUFA production', *PUFAChain*, p. 79, 2017.
- [53] R. Saini, K. Hegde, C. S. Osorio-gonzalez, S. K. Brar, and P. Vezina, 'Evaluating the Potential of *Rhodospiridium toruloides*-1588 for High Lipid Production Using Undetoxified Wood Hydrolysate as a Carbon Source', *Energies*, vol. 13, pp. 2–14, 2020.

- [54] S. N. Naik, V. V Goud, P. K. Rout, and A. K. Dalai, 'Production of first and second generation biofuels : A comprehensive review', vol. 14, pp. 578–597, 2010.
- [55] A. E. Atabani, A. S. Silitonga, I. Anjum, T. M. I. Mahlia, H. H. Masjuki, and S. Mekhilef, 'A comprehensive review on biodiesel as an alternative energy resource and its characteristics', *Renew. Sustain. Energy Rev.*, vol. 16, no. 4, pp. 2070–2093, 2012.
- [56] B. R. Moser, 'Biodiesel Production, Properties, and Feedstocks', *Vitr. Cell.Dev.Biol.-Plant*, vol. 45, pp. 229–266, 2009.
- [57] G. Huang, F. Chen, D. Wei, X. Zhang, and G. Chen, 'Biodiesel production by microalgal biotechnology', *Appl. Energy*, vol. 87, no. 1, pp. 38–46, 2010.
- [58] B. Han, H. Goh, H. Chyuan, M. Yee, W. Chen, and K. Ling, 'Sustainability of direct biodiesel synthesis from microalgae biomass : A critical review', *Renew. Sustain. Energy Rev.*, vol. 107, no. May 2018, pp. 59–74, 2019.
- [59] D. Singh, D. Sharma, S. L. Soni, S. Sharma, P. Kumar Sharma, and A. Jhalani, 'A review on feedstocks, production processes, and yield for different generations of biodiesel', *Fuel*, vol. 262, no. July, 2020.
- [60] D. P. Ho, H. H. Ngo, and W. Guo, 'A mini review on renewable sources for biofuel', *Bioresour. Technol.*, vol. 169, no. July, pp. 742–749, 2014.
- [61] X. Meng, J. Yang, X. Xu, L. Zhang, Q. Nie, and M. Xian, 'Biodiesel production from oleaginous microorganisms', *Elsevier*, vol. 34, pp. 1–5, 2009.
- [62] M. Aminul, K. Heimann, and R. J. Brown, 'Microalgae biodiesel: Current status and future needs for engine performance and emissions', *Renew. Sustain. Energy Rev.*, vol. 79, pp. 1160–1170, 2017.
- [63] CEN, 'Automotive fuels — Fatty acid methyl esters (FAME) for diesel engines — Requirements and test methods', 2010.
- [64] T. Lopes and A. Reis, *Scale-up Problems for the Large Scale Production of Algae Scale-up Problems for the Large Scale Production of Algae*, D. Das (ed., no. December 2016. Springer International Publishing, 2015.
- [65] T. Lopes Da Silva and A. Reis, 'The use of multi-parameter flow cytometry to study the impact of n-dodecane additions to marine dinoflagellate microalga *Cryptocodinium cohnii* batch fermentations and DHA production', *J. Ind. Microbiol. Biotechnol.*, vol. 35, no. 8, pp. 875–887, 2008.
- [66] T. L. da Silva, J. C. Roseiro, and A. Reis, 'Applications and perspectives of multi-parameter flow cytometry to microbial biofuels production processes', *Trends Biotechnol.*, vol. 30, no. 4, pp. 225–232, 2012.

- [67] M. Díaz, M. Herrero, L. A. García, and C. Quirós, *Flow Cytometry: A High-Throughput Technique for Microbial Bioprocess Characterization*, Second Edi., vol. 2. Elsevier B.V., 2011.
- [68] A. De Jara, A. Martel, C. Molina, L. Nordström, V. De Rosa, and D. Ricardo, 'Flow cytometric determination of lipid content in a marine dinoflagellate , *Cryptothecodinium cohnii*', *J. Appl. Phycol.*, vol. 15, pp. 433–438, 2003.
- [69] A. L. Guide, *Introduction to Flow Cytometry* : 2000.
- [70] C. Series, 'Instructions for Use CytoFLEX Series', no. July, 2018.
- [71] K. Goda, 'Compensation in Multicolor Flow Cytometry', *Cytometry. A*, vol. 87, no. 11, pp. 8–11, 2015.
- [72] H. Pereira, P. S. C. Schulze, L. M. Schüler, T. Santos, L. Barreira, and J. Varela, 'Fluorescence activated cell-sorting principles and applications in microalgal biotechnology', *Algal Res.*, vol. 30, pp. 113–120, 2018.
- [73] Y. Wang, F. Hammes, K. De Roy, W. Verstraete, and N. Boon, 'Past, present and future applications of flow cytometry in aquatic microbiology', *Cell Press*, vol. 28, pp. 416–424, 2010.
- [74] C. Quirós, M. Herrero, L. A. García, and M. Díaz, 'Application of flow cytometry to segregated kinetic modeling based on the physiological states of microorganisms', *Appl. Environ. Microbiol.*, vol. 73, no. 12, pp. 3993–4000, 2007.
- [75] A. Microbiol, G. G. Satpati, and R. Pal, 'Rapid detection of neutral lipid in green microalgae by flow cytometry in combination with Nile red staining — an improved technique', *Ann Microbiol*, vol. 65, pp. 937–949, 2014.
- [76] M. Chioccioli, B. Hankamer, and I. L. Ross, 'Flow cytometry pulse width data enables rapid and sensitive estimation of biomass dry weight in the microalgae *Chlamydomonas reinhardtii* and *Chlorella vulgaris*', *PLoS One*, vol. 9, no. 5, pp. 1–12, 2014.
- [77] T. Tabora, 'Using low-cost carbon sources for the production of biodiesel and omega-3 lipids from the heterotrophic microalgae *Cryptothecodinium cohnii*', Instituto Superior Técnico, 2019.
- [78] S. Sousa, 'Produção microbiana de lípidos e carotenóides em culturas da levedura *Rhodospiridium toruloides* NCYC 921 desenvolvidas em regime semi-descontínuo', Instituto Superior Técnico, 2014.
- [79] G. E. Marti, M. Stetler-Stevenson, J. J. H. Bleasing, and T. A. Fleisher, *Introduction to flow cytometry*, vol. 38, no. 2. 2001.
- [80] 'CytoFLEX Flow Cytometer Platform', *Beckman Coulter Life Sci.*, p. 14, 2019.
- [81] Olympus, 'Instructions BX60 System Microscope', 2021. [Online]. Available: <https://www.manualslib.com/products/Olympus-Bx60-8988361.html>.

- [82] W. E. Federation, '4500-Norg NITROGEN (ORGANIC)', *Stand. Methods Exam. Water Wastewater*, no. 1, pp. 130–135, 1999.
- [83] M. J. Pratas, S. V. D. Freitas, M. B. Oliveira, S. C. Monteiro, and S. Lima, 'Biodiesel Density : Experimental Measurements and Prediction Models', *Energy and Fuels*, vol. 25, pp. 2333–2340, 2011.
- [84] S. V. D. Freitas, M. J. Pratas, R. Ceriani, and A. P. Coutinho, 'Evaluation of Predictive Models for the Viscosity of Biodiesel', no. 14, pp. 352–358, 2011.
- [85] E. G. Giakoumis and C. K. Sarakatsanis, 'A comparative assessment of biodiesel cetane number predictive correlations based on fatty acid composition', *Energies*, vol. 12, no. 3, pp. 1–30, 2019.
- [86] S. Mishra, K. Anand, and P. S. Mehta, 'Predicting the Cetane Number of Biodiesel Fuels from Their Fatty Acid Methyl Ester Composition', *Energy and Fuels*, vol. 30, no. 12, pp. 10425–10434, 2016.
- [87] M. E. De Swaaf, T. C. De Rijk, G. Eggink, and L. Sijtsma, 'Optimisation of docosahexaenoic acid production in batch cultivation by *Cryptocodinium cohnii*', *Elsevier*, vol. 70, pp. 185–192, 1999.
- [88] T. Lopes and Æ. A. Reis, 'The use of multi-parameter flow cytometry to study the impact of n - dodecane additions to marine dinoflagellate microalga *Cryptocodinium cohnii* batch fermentations and DHA production', *J. Ind. Microbiol. Biotechnol.*, vol. 35, pp. 875–887, 2008.
- [89] P. Ka *et al.*, 'Involvement of calcium mobilization from caffeine-sensitive stores in mechanically induced cell cycle arrest in the dinoflagellate *Cryptocodinium cohnii*', *Elsevier*, vol. 39, pp. 259–274, 2006.
- [90] Z. Y. Wen and F. Chen, 'Heterotrophic production of eicosapentaenoic acid by the diatom *Nitzschia laevis*: Effects of silicate and glucose', *J. Ind. Microbiol. Biotechnol.*, vol. 25, no. 4, pp. 218–224, 2000.
- [91] F. Chen and M. R. Johns, 'Effect of C/N ratio and aeration on the fatty acid composition of heterotrophic *Chlorella sorokiniana*', *J. Appl. Phycol.*, vol. 3, no. 3, pp. 203–209, 1991.
- [92] Gudmundur G. Haraldsson Bjorn Kristinsson, 'Process for separating polyunsaturated fatty acids from long chain unsaturated or less saturated fatty acids', *European Patent Office*, 2011. [Online]. Available: <https://patents.google.com/patent/EP2585570A1/en>.
- [93] T. Lopes da Silva, A. R. Santos, R. Gomes, and A. Reis, 'Valorizing fish canning industry by-products to produce ω -3 compounds and biodiesel', *Environ. Technol. Innov.*, vol. 9, pp. 74–81, 2018.
- [94] F. Fabu, 'Fatty acid molecular weights', *Danish Food Inf.*, pp. 1–7, 2011.
- [95] N. M. C. T. Prieto, A. G. M. Ferreira, R. J. Moreira, and J. B. Santos, 'Correlation and prediction of biodiesel density for extended ranges of temperature and pressure', *FUEL*, vol. 141, pp. 23–

38, 2015.

[96] Y. Chisti, 'Biodiesel from microalgae', *Biotechnol. Adv.*, vol. 25, no. 3, pp. 294–306, 2007.

Appendix A

Table A.1 - Chemical reagents used in this work.

Name	Chemical Formula	Purity (%)	Brand	Application
Sea salt	Sea Salt	-	OceanusIberica	Growth Medium
Yeast Extract Powder	-	-	HiMedia	Growth Medium
Chloramphenicol	$C_{11}H_{12}Cl_2N_2O_5$	99.4	USB	Growth Medium (antibiotic)
Penicillin G sodium salt	$C_{16}H_{17}N_2NaO_4S$	-	AlfaAesar	Growth Medium (antibiotic)
Streptomycin Sulfate	$(C_{21}H_{39}N_7O_{12})_2 \cdot 3H_2SO_4$	-	PanReac	Growth Medium (antibiotic)
Sodium hydroxide	NaOH	-	José M. Vaz Pereira, S.A.	Residual nitrogen (Kjeldahl method) / Growth Medium (pH adjustments)
Hydrochloric acid	HCl	-	Merck	Growth Medium (pH adjustments)
Polypropylene glycol	-	-	Prolab	Growth Medium (anti-foaming agent)
Sulphuric acid	H_2SO_4	97.0	Merck	HPLC
CFDA	$C_{29}H_{19}NO_{11}$	-	Life Technologies	Flow Cytometry
Propodium Iodide	$C_{27}H_{34}I_2N_4$	-	Life Technologies	Flow Cytometry
Boric acid	H_3BO_3	99.8	Merck	Residual nitrogen (Kjeldahl method)

Table A.2 (continuation) - Chemical reagents used in this work.

Name	Chemical Formula	Purity (%)	Brand	Application
Methanol	CH ₃ OH	99.8	Merck	Lipid Analysis (Transmethylation)
Acetyl chloride	C ₂ H ₃ ClO	98.5	Panreac	Lipid Analysis (Transmethylation)
Heptadecanoic acid	C ₁₇ H ₃₄ O ₂	-	Nu-Check-Prep	Lipid Analysis (Internal Standard)
N-heptane	C ₇ H ₁₆	99.0	Fisher Chemical	Lipid Analysis (FAME Extraction)
Sodium sulfate, anhydrous	Na ₂ SO ₄	99.0	Merck	Lipid Analysis (FAME Extraction)
Petroleum Ether (80-110 °C)	-	-	Chem-Lab	Lipid Analysis (Dissolution of 17:0)
D-Glucose, anhydrous	C ₆ H ₁₂ O ₆	99.5	Pronolab	Growth Medium

Appendix B

The following regression equations, (20), (21) and (22) were obtained from measurements – Experiment I, II and III:

$$\text{OD}_{470} = 8\text{E-}07 * \text{Cell number (cells/mL)} - 0.1245 \quad R^2 = 0.992 \quad (20)$$

$$\text{DCW (g/L)} = 9\text{E-}07 * \text{Cell number (cells/mL)} - 0.4133 \quad R^2 = 0.991 \quad (21)$$

$$\text{DCW (g/L)} = 1.0889 * \text{OD}_{470} - 0.2497 \quad R^2 = 0.983 \quad (22)$$

Appendix C

Table A.1 - Requirements of biodiesel properties according to the European standard EN 14214.

Property	Minimum	Maximum	Unit
Ester content	96.5	-	%(w/w)
Density at 15°C	860	900	kg/m ³
Kinematic Viscosity at 40°C	3.5	5.0	mm ² /s
Flash point	> 101	-	°C
Sulfur content	-	10	mg/kg
Cetane number	51	-	-
Sulfated ash content	-	0.02	%(w/w)
Water content	-	500	mg/kg
Total contamination	-	24	mg/kg
Copper band corrosion (3 hours at 50 °C)	Class 1	Class 1	rating
Oxidation stability, 110°C	6	-	hours
Acid value	-	0.5	mg KOH/g
Iodine value	-	120	-
Linolenic Acid methyl ester	-	12	%(w/w)
Polyunsaturated (≥ 4 Double bonds) methyl ester	-	1	%(w/w)
MeOH content	-	0.2	%(w/w)

Table A.2 (continuation)- Requirements of biodiesel properties according to the European standard EN 14214.

Property	Minimum	Maximum	Unit
Monoglyceride content	-	0.7	%(w/w)
Diglyceride content	-	0.2	%(w/w)
Triglyceride content	-	0.2	%(w/w)
Free glycerol	-	0.02	%(w/w)
Total glycerol	-	0.25	%(w/w)
Alkaline Metals (Na⁺ K⁺)	-	5	mg/kg
Phosphorus content	-	4	mg/kg